

## Article

# Method of Evaluation of Materials Wear of Cylinder-Piston Group of Diesel Engines in the Biodiesel Fuel Environment

Magdalena Kaplan <sup>1</sup>, Kamila Klimek <sup>2</sup>, Grzegorz Maj <sup>3</sup>, Dmytro Zhuravel <sup>4</sup>, Andrii Bondar <sup>4</sup>, Viktoriia Lemeshchenko-Lagoda <sup>4</sup>, Boris Boltianskyi <sup>4</sup>, Larysa Boltianska <sup>4</sup>, Hanna Syrotyuk <sup>4</sup>, Serhiy Syrotyuk <sup>5</sup>, Ryszard Konieczny <sup>6</sup>, Gabriel Filipczak <sup>7</sup>, Dorota Anders <sup>8,9</sup>, Barbara Dybek <sup>8,9</sup> and Grzegorz Wałowski <sup>8,9,\*</sup>

<sup>1</sup> Department of Pomology, Nursery and Enology, University of Life Sciences in Lublin, 28 Gleboka Street, 20-612 Lublin, Poland; magdalena.kaplan@up.lublin.pl

<sup>2</sup> Department of Applied Mathematics and Computer Science, University of Life Sciences in Lublin, 28 Gleboka Street, 20-612 Lublin, Poland; kamila.klimek@up.lublin.pl

<sup>3</sup> Department of Power Engineering and Transportation, University of Life Sciences in Lublin, 28 Gleboka Street, 20-612 Lublin, Poland; grzegorz.maj@up.lublin.pl

<sup>4</sup> Department of Technical Systems and Technology in Livestock, Dmytro Motorny Tavria State Agrotechnological University, 18 Bohdana Khmelnytskoho Avenue, Zaporizhia Oblast, 72312 Melitopol, Ukraine; dmytro.zhuravel@tsatu.edu.ua (D.Z.); andrii.bondar@tsatu.edu.ua (A.B.); viktoriia.lemeshchenko@tsatu.edu.ua (V.L.-L.); boris.boltianskyi@tsatu.edu.ua (B.B.); larysa.boltianskai@tsatu.edu.ua (L.B.); hanna.syrotyuk@tsatu.edu.ua (H.S.)

<sup>5</sup> Department of Energy, Lviv National Agrarian University, 1 V. Velykoho Street, 80381 Dubliany, Ukraine; ssyr@ukr.net

<sup>6</sup> Department of Technology, Institute of Energy and Technical Safety, Jacob of Paradyz University, 52 Chopina Street, 66-400 Gorzow Wielkopolski, Poland; rkonieczny@ajp.edu.pl

<sup>7</sup> Department of Process and Environmental Engineering, Faculty of Mechanical Engineering, Opole University of Technology, 5 Mikołajczyka Street, 45-271 Opole, Poland; g.filipczak@po.edu.pl

<sup>8</sup> Institute of Technology and Life Sciences—National Research Institute, Falenty, Al. Hrabaska 3, 05-090 Raszyn, Poland; d.anders@itp.edu.pl (D.A.); b.dybek@itp.edu.pl (B.D.)

<sup>9</sup> Department of Technology, Branch Poznan, 67 Biskupinska Street, 60-463 Poznan, Poland

\* Correspondence: g.walowski@itp.edu.pl



**Citation:** Kaplan, M.; Klimek, K.; Maj, G.; Zhuravel, D.; Bondar, A.; Lemeshchenko-Lagoda, V.; Boltianskyi, B.; Boltianska, L.; Syrotyuk, H.; Syrotyuk, S.; et al.

Method of Evaluation of Materials Wear of Cylinder-Piston Group of Diesel Engines in the Biodiesel Fuel Environment. *Energies* **2022**, *15*, 3416. <https://doi.org/10.3390/en15093416>

Academic Editors: Patrick Hendrick and Diego Luna

Received: 29 March 2022

Accepted: 5 May 2022

Published: 7 May 2022

**Publisher's Note:** MDPI stays neutral with regard to jurisdictional claims in published maps and institutional affiliations.



**Copyright:** © 2022 by the authors. Licensee MDPI, Basel, Switzerland. This article is an open access article distributed under the terms and conditions of the Creative Commons Attribution (CC BY) license (<https://creativecommons.org/licenses/by/4.0/>).

**Abstract:** This article concerns the method of material consumption assessment of the cylinder-piston group of diesel engines in the biodiesel environment. The obtained experimental dependences of the wear coefficients on the example of the tribounit cylinder liner and the piston ring can be used to forecast the resource use during operation under specific conditions of the engine and the environment as a whole. The article systematizes the types of biofuels, depending on the type of raw materials from which they were made, taking into account the process and application. The physical and chemical aspects of the catalysts used for biofuels were indicated. The applied experimental methods for tribological wear of the piston-cylinder pair were analyzed. B70 biodiesel was used in the research, i.e., 70% mineral diesel oil and 30% methyl esters of rapeseed oil. Experimental tribotechnical studies of the influence of biofuels on the behavior of various materials have shown that when using this type of fuel, it is necessary to replace the materials from which some parts of the cylinder-piston group are made. To solve this problem, research has been carried out on a specially designed friction machine. The novelty in the article concerns the association, based on the literature, of hydrogen consumption causing material wear in friction contacts. The mechanism of the interaction of various construction materials during such friction has been disclosed.

**Keywords:** biodiesel; agricultural machinery; antiwear properties; diesel engine; wear; cylinder-piston group; tribotechnical

## 1. Introduction

In 2012, the European Commission adopted a strategy for the sustainable use of renewable resources in the European economy called “Innovation for Sustainable Growth:

A Bioeconomy for Europe” [1]. This strategy highlights the need to develop the production of renewable raw materials in Europe. The aim of the EU strategy is to lay the foundations for an innovative and thus competitive economy in which the use of renewable resources for industrial purposes is one of the basic assumptions [2].

The essence of bioeconomy is the management of renewable biological resources (plants, animals and microorganisms), with the support of such fields as biotechnology, biology, chemistry, ecology, nanotechnology, medical and economic sciences for the production of traditional and new products with high added value, e.g., food, feed, bioproducts and bioenergy [3]. Bioeconomy meets the requirements of smart specialization, represents various areas of activity from various sectors of the economy, technologies and processes, and is in line with the main priorities of the Europe 2020 strategy [4].

The term bioeconomy is defined as a set of sectors of the economy that deal with the production, processing and use of resources of biological origin [5]. However, in the report “The Knowledge Based Bio-Economy (KBBE) in Europe: Achievements and Challenges”, the bioeconomy was defined as the sustainable production and conversion of biomass in relation to food, health, fibers, industrial products and energy, where renewable biomass resources are any biological material that can be used as a raw material [6]. The bioeconomy sectors are agriculture, forestry, food industry, fishing, chemical, pharmaceutical, cosmetic and textile industries, as well as energy production based on the use of biomass as the main raw material. The primary function of the bioeconomy is to produce various types of bio-based products by using renewable biological resources. The analysis of different definitions of bioeconomy showed that the common denominator of all definitions is the use of natural resources in the production process [7] and their transformations [8].

Biofuels produced from biomass for transport have become one of the most promising types of alternative and environmentally friendly fuels, which can, to some extent, replace petrol and diesel oil (ON) [9]. Biofuel is an ambiguous term, presenting different interpretations of the base concept, covering a very wide range of different substrates. Liquid or gaseous biofuels are an alternative to ON, as they are produced with an admixture of plant biocomponents (rape, soybean, sunflower, palm oil and other oil plants), which contributes to the reduction of the use of petroleum fuels [10].

In the Americas, ethanol is very popular; it is produced from plants rich in sugar or starch (in Brazil it is made from sugar cane, in the USA from corn). Diesel biofuels, more popular in Europe, are produced from oils and fats. Both types of fuel can be used clean, in appropriately adapted engines, or they can be components of a mixture, together with diesel fuel or gasoline. The production technologies of biofuels vary in terms of the raw material used in the production process, as shown in Table 1.

**Table 1.** Types of biofuels, depending on the type of raw materials from which they were made [own study].

Substrate	Production-Group	Production-Subgroup	Process Use Net Calorific Value	Process Use	Net Calorific Value
First generation biofuels					
Arable crops such as cereals, corn, sugar cane, rape, sugar beets	Bioethanol (alcoholic fermentation)	Bioethanol (BioEtOH) understood as conventional ethanol [11]	Hydrolysis and fermentation of sugars	Car engines	27 MJ/kg
		Pure Vegetable Oils (PVO)	Cold pressing and extraction of oilseeds	Only in suitably modified diesel engines [12]	37 MJ/kg
	Biodiesel (1st generation) esterification of vegetable oils: –rapeseed, –soy, –palm, –sunflower	Biodiesel being methyl esters (Fatty Acid Methyl Esters-FAME) and ethyl (Fatty Acid Ethylesters-EAEE) higher fatty acids of oilseeds, including rapeseed (Rapeseed Methyl Ester-RME, REE)	Cold pressing, extraction and transesterification	diesel fuel; Fuel with an appropriate additive quantity and quality of the biocomponent [13]	37 MJ/kg 40.1 MJ/kg
		biodiesel, being methyl and ethyl esters	Transesterification post-cooking oil waste and animal fats		
	Biogas		Cleaning of landfill or agricultural biogas;	Cogeneration	20–26 MJ/m <sup>3</sup>

Table 1. Cont.

Substrate	Production-Group	Production-Subgroup	Process Use Net Calorific Value	Process Use	Net Calorific Value
Second generation biofuels					
Organic cellulose residues, derived from plants that can be grown in wastelands or polluted areas (straw, energy willow, miscanthus)	Bioethanol, obtained as a result of advanced hydrolysis and fermentation processes of cellulose and lignocellulosic biomass (excluding foodstuffs)	Ethyl alcohol (BioEt) and ethyl-tert-butyl esters (Ethyl-Tert-Butyl Ether–ETBE) obtained from BioEt; HTU-diesel fuel (Hydro Thermal Upgrading) obtained in the process of depolymerization of waste organic raw materials at high temperature, the so-called pyrolytic hydrothermal decomposition of biomass;	Extraction, pyrolysis, synthesis, synthetic hydrolysis as well as hydrotreatment	Additive to motor gasoline, as bio-additive E%, e.g., E95 containing 95% gasoline and 5% ethanol [12,14].	27 MJ/kg
	Synthetic biofuels, which are products of biomass processing waste and lignocellulosic by gasification and appropriate synthesis into liquid components fuel (Biomass to Liquid-BtL [15])	Biohydrogen	Gasification of lignocellulose and synthesis of the resulting products, or a biochemical process	Production: –thermal energy, –electricity in fuel cells, –intrinsic motor fuel	43 MJ/kg
	hydrocarbon fuels for ignition engines self-acting obtained by the Fischer-Tropsch processes	Synthetic hydrocarbon fuels	Gasification	BtL –liquid fractions and mixtures obtained from biomass	44 MJ/kg
	Biomethanol;	It is chemically identical to standard methanol.	Dry distillation of plant biomass, consisting in drying and grinding the raw material and introducing the obtained pulp into the reactor and gasification	A fuel replacement for aviation and sport spark ignition engines and as a solvent [16].	20 MJ/kg
	Mixtures Higher alcohols and dimethyl ether (bio-DME);		Dimethyl ether is produced from synthesis gas (CO + H <sub>2</sub> ) by two methods: indirect synthesis (via methanol) and direct synthesis [17]	Car transport	28 MJ/kg
	Dimethylfuran (DMF)		A solvent used in many industrial sectors, in particular chemical	–dyes, laboratory chemicals, –cleaning products, –adhesives and sealants	28 MJ/kg
Biogas and the biomass liquefaction process, during which it is first gasified	Biogas	Biological breakdown of organic materials in an anaerobic atmosphere known as anaerobic breakdown The power-to-gas process allows the captured CO <sub>2</sub> to be utilized and transformed into a usable fuel which is SNG		The gas obtained is then used to produce fuels	17–25 MJ/m <sup>3</sup>
	SNG (Synthetic Natural Gas)–synthetically obtained natural gas;				

Table 1. Cont.

Substrate	Production-Group	Production-Subgroup	Process Use Net Calorific Value	Process Use	Net Calorific Value
Non-food oils [18]: –cooking oils, –oils from inedible plants, –jatropha, jojoba			HVO–Hydrotreated Vegetable Oil–hydrothermal catalysis, hydrogenation, hydrotreatment (co-hydrogenation) of components from oil processing petroleum and vegetable oils and/or animal fats	Under combustion conditions of partially homogeneous mixtures (ang. Partially Premixed Compression Ignition)	
	Biodiesel (2nd generation)		HTU–Hydrothermal Upgrading–pyrolytic hydrothermal decomposition of biomass with water at 300–350 °C and 100–180 bar pressure within 5–15 min [19] chemical catalysis-acidic and alkaline, at what sour technologies are less efficient (slower) but require lower temperatures (up to 60 °C), making them less energy-intensive (alkaline catalysis requires approx. 80 °C) [19] Enzymatic with the use of lipases (enzymes that break down fats) produced by certain strains of bacteria [21]	Jet fuel with hydrotreated esters or acids fatty [20]  Renewable jet fuel [20]  Jet fuel from fermentation advanced [20]	40.1 MJ/kg
Biomass					
Third generation biofuels					
Algae-reserve substances: starch and lipids, and building substances: protein contained in cells of some species.	Biodiesel (3rd generation)	A source of several types of renewable biofuels, incl. biodiesel, biohydrogen and biomethane	30 times more energy than from 1st or 2nd generation biofuels [22]	Hydrogen production servant to power fuel cells [23]	120 MJ/kg

From an ecological point of view, the main advantage of biodiesel as a fuel is combustion with less exhaust gas. Compared to pure diesel fuel, the combustion of esters is associated with lower CO and CO<sub>2</sub> emissions, and the amount of solid particles and the amount of hydrocarbons in the exhaust gas are also reduced (there is less soot and a lower smoke level). FAME, due to its plant origin, contains practically no sulfur (about 300 times less than is in diesel fuel) [24].

Diesel engines are not only power units for vehicles, but also work as stationary power generators [25–27]. Due to high thermal efficiency and small dimensions, diesel engines have been widely used [28,29]. Alternative fuels are sought to reduce the emission of harmful components from exhaust gases [30–32]. In response to the depletion of mineral resources and the increase in CO<sub>2</sub> emissions as a result of the combustion of mineral fuels, research is conducted around the world on the production of fuels from biomass of various origins [33–35]. Liquid fuels obtained from the indicated sources in the form of biodiesel of various qualities [36–38] are an important source of energy that can be used locally by their producers for their own needs [39]. A special case to be considered in the

sustainable development policy are entities producing various types of biofuels and using biodiesel to produce electricity in a dual-fuel internal combustion engine driving an electric generator [40,41]. This solution significantly reduces the farm's demand for energy from external sources and increases its independence from the indicated energy sources [42].

Modern research focuses on the search for new catalysts for transesterification, i.e., heterogeneous or homogeneous (liquid) catalysts—depending on the type of catalyst (magnetic nanoparticles, ionic liquids, sulfonated carbon). The production of biodiesel itself also uses different substrates, so production efficiency can also be compared in terms of oil type. Research is also carried out on noncatalytic transesterification systems.

The biocatalyst has shown a high benefit for biodiesel production under mild conditions. A typical catalyst was able to efficiently convert soybean oil into biodiesel; the biodiesel yield was almost 1.5 times higher. The catalyst retained approximately 80% activity throughout the process—this study provided an effective strategy for regulating hydrophobicity and surface support potential to increase the efficiency of immobilized lipase [43]. A novel ionic liquid magnetic catalyst has been developed to generate alternative biodiesel energy using cress seed oil. The heterogeneous catalyst showed high catalytic efficiency that reached 92.38% biodiesel yield. The prepared catalyst retained excellent catalytic parameters, which meant that the produced biodiesel could be used for biofuel as an ideal substitute. The oil consisted of a total of 12 fatty acids that contained 4.18% of saturated fatty acids (SFA)—72.29% [44].

Four types of ionic liquids were synthesized in the study and used for one-step transesterification of wet microalgae to fatty acid methyl esters (FAME) in the presence of methanol as refined oils (sunflower, rapeseed and corn oils). Optimized conditions gave a yield of 98% using biomass containing 40% water by weight. Finally, it was confirmed that the ionic liquid can be reused and recycled with less than 2% loss between cycles. Due to its simplicity and low cost of synthesis, it is a promising catalyst for the transesterification process for the production of biodiesel from wet microalgae biomass. The leading candidate ionic liquid catalyst, tetrabutylphosphonium formate, was further optimized using response surface methodology to minimize material consumption, increase water compatibility and reduce processing time while maximizing yield from wet microalgae biomass [45].

The synthesis of magnetic material allowed for the use of a magnetic field to combine the catalytic function of acid-base ionic liquid with silicon for biodiesel production. A kind of magnetic catalyst with immobilized ionic liquid was synthesized by a three-step method. The synthesis conditions were optimized at each stage by means of one-way analysis. The biodiesel yield was 0.557 g/g (catalyst yield approx. 89.2%). Catalytic efficiency was 87.6% of the first one used after four reusing cycles. The stirring speed is an extremely important factor that can affect the particle size and the specific surface area of the catalyst surface and increasing the specific surface area will indirectly affect the binding amount of the ionic liquid; however, when the stirring speed reaches a certain speed, the binding amount has little effect. In this experiment, a stirrer with a stepless speed was used. As the speed increased from 250 to 350 rpm, the product yield increased by 22.7%. Above 350 rpm, the increase in  $\text{Fe}_3\text{O}_4@\text{SiO}_2$  yield was minimal (1.21%). According to these results, a rotational speed of 350 rpm was selected for subsequent experiments. As the TEOS volume increased, the yield of  $\text{Fe}_3\text{O}_4@\text{SiO}_2$  also increased. The maximum silica gel layer thickness was not reached if the TEOS volume was insufficient. Consequently, the silica gel adhesion was improved, and the product yield increased with the increase of TEOS volume. When the TEOS volume exceeded 5 mL, the amount loaded on  $\text{Fe}_3\text{O}_4@\text{SiO}_2$  hardly increased because TEOS was present in excess. When the weight of  $\text{Fe}_3\text{O}_4$  was 1.5 g, the optimal volume of TEOS was 5 mL [46].

The study produced new nanocomposites based on a magnetic ionic liquid. The engineered nanocomposites were used as a catalyst for the transesterification of palm oil for biodiesel production. The results showed better performance under biodiesel performance conditions; the maximum efficiency is 86.4%. The results revealed that  $[\text{NiFe}_2\text{O}_4@\text{BMSI}]\text{HSO}_4$  showed better performance in terms of biodiesel performance;

the maximum, i.e., 86.4%, efficiency was obtained using  $[\text{NiFe}_2\text{O}_4@\text{BMSI}]\text{HSO}_4$ , while in the case of  $[\text{NiFe}_2\text{O}_4@\text{BMSI}]\text{Br}$ , the efficiency of about ~74.6% was obtained at 5% (w/w) catalyst load, 353 K and a ratio to  $\text{CH}_3\text{OH}$  of 1:12 within 8 h. Catalyst reuse results showed that catalyst catalytic activity still remained at around 92.7% and 88.1% with  $[\text{NiFe}_2\text{O}_4@\text{BMSI}]\text{HSO}_4$  and  $[\text{NiFe}_2\text{O}_4@\text{BMSI}]\text{Br}$ , respectively, after six cycles, which can be attributed to handling losses during process manipulation [47].

A nano-size magnetic solid catalyst from ash biowaste from *Citrus sinensis* shells was developed for the synthesis of biodiesel from waste cooking oil. The core-shell structure of the catalyst improved the surface properties and maintained control over the size and shape of the catalyst, so that the stability of the catalyst was significantly improved. Catalyzed transesterification provided a maximum biodiesel yield of 98% under optimized conditions. The catalyst showed high physical stability and reactivity for up to nine consecutive cycles, proving to be a promising solid-based catalyst for sustainable biodiesel production. Transesterification catalyzed by  $\text{CSPA}@\text{Fe}_3\text{O}_4$  gave a maximum biodiesel yield of 98% under optimized reaction conditions such as a methanol/oil molar ratio of 6:1, 6% weight loading of catalyst, temperature of 65 °C and time of 3 h. The activation energy of the reaction was found to be 34.41  $\text{KJ mol}^{-1}$ , indicating that the transesterification of WCO using the present catalyst is a chemically controlled reaction. [48].

Magnetic mesoporous acid catalysts are designed for the production of biodiesel by transesterification of palm oil with methanol. The catalyst was very efficient in transesterifying palm oil with methanol and gave more than 91% biodiesel efficiency after six cycles, making the catalyst an excellent prospect for industrial applications. The results indicated that everyone ordered mesoporous and excellent paramagnetic. Both  $\text{Fe}_3\text{O}_4@\text{SBA-15}@\text{HPW}$  and  $\text{Fe}_3\text{O}_4@\text{SBA-15-NH}_2\text{-HPW}$  were characterized by a high content of Brønsted acid centers because of the charge of 12-tungsten acid, which made both catalysts very active. In particular,  $\text{Fe}_3\text{O}_4@\text{SBA-15-NH}_2\text{-HPW}$  was very efficient at transesterifying palm oil with methanol and gave more than 91% of the biodiesel yield when the reaction was carried out at 150 °C from 4% by weight. The catalyst in 20 molar ratio methanol/oil:1 for 5 h  $\text{Fe}_3\text{O}_4@\text{SBA-15-NH}_2\text{-HPW}$  produced by the grafting method showed greater reusability, and the biodiesel efficiency after six cycles was over 80%, which made the catalyst an excellent prospect for industrial application [49].

In this study, a novel acidic carbon catalyst was synthesized by carbonization of deoiled microalgae biomass followed by sulfonation. The effects of catalyst synthesis conditions such as carbonization temperature, sulfonation time and  $\text{H}_2\text{SO}_4$  concentration on catalyst surface acidity and free fatty acid conversion were determined. The solid acid catalyst (DMB) based on deoiled microalgal biomass was mainly composed of carboxyl, phenolic and sulfonic groups as indicated by FTIR analysis and supported by XPS analysis. The catalyst was then characterized by various methods to determine its physicochemical properties. The maximum yield of fatty acid methyl esters (FAME) is 94.23% for microalgae oil and 96.25% for kitchen waste; the oil was obtained under optimized transesterification conditions. The catalyst showed high catalytic activity (FAME yield > 90%) until the fourth cycle. Most of the biodiesel properties were within the limits of EN 14212 and ASTM D6751 [50].

From the refining of rice bran oil, the fatty acid distillate of rice bran oil is a low-value, inedible and undesirable by-product that can be used as a promising alternative feedstock for biodiesel production. A high quality of biodiesel and a valuable by-product (glyoxal) was obtained. In this process, 80.9% biodiesel content was achieved as a raw material, compared to only 43.6% for refined rice bran oil as a raw material. The biodiesel content of 97.1% was achieved under optimal conditions—these results provided new insight into the development of biodiesel production from low-quality feedstocks. In this paper, biodiesel synthesis was performed in a microreactor under supercritical DMC conditions. First, RBOFAD (or refined RBO) was pre-mixed with DMC in the desired ratio (molar ratio of DMC to oil between 1.8:1 and 25.7:1) in the beaker to obtain a homogeneous substrate solution. The RBOFAD (or sophisticated RBO) and DMC stream were then introduced

into the microreactor using an HPLC pump (LKB Bromma 2150) at the desired residence time (8 to 67 min). The microreactor in which the transesterification/esterification reactions occurred was placed inside a convection oven (adapted from a gas chromatography oven; Varian 3600) to control the reaction temperature (275 to 375 °C). The reactor outlet was connected to a backpressure regulator to control the pressure at 8 MPa [51].

The efficiency of the aviation fuels obtained from lipids in six vegetable oils (olive, coconut, soybean, rapeseed, avocado and sesame) was investigated. The noncatalytic conversion platform led to the conversion of vegetable oils into biodiesel with an efficiency of more than 90% at 380 °C in 1 min, while the base-catalyzed reaction with KOH showed the same efficiency after 8 h of reaction at 60 °C. The ideal gas turbine cycle of a turbojet aircraft was used to calculate the fuel efficiency for biodiesel jet engines from the non-catalytic transesterification of six vegetable oils. As a reference, the performance of conventional jet fuels (Jet A and JP-4) by a turbojet engine with a constant air supply was estimated. For the complete combustion of fuels, biodiesels required 14 to 18% more fuel consumption than conventional jet fuels [52].

One of the main problems with biodiesel standardization is the complex development of methods for determining its quality indicators. While the well-known methods, which have long been used in Ukraine on inexpensive and common equipment, can be applied to physical quality indicators, most chemical indicators require the introduction of new special methods. It is necessary to develop several methodologies, differentiating them according to the complexity and accuracy of the analysis. Important factors for the growth of biodiesel production, apart from technical and economic ones, are excellent functional properties and environmental safety of this type of fuel. However, the relevant regulations must be observed during use, transport and storage. They should be regularly improved in line with changes in the legal and regulatory framework, the appearance of new engines, construction materials, additives and other applications.

The advantages of biodiesel over other energy sources are that biodiesel is made from renewable resources; its chemical properties are very similar to oils. The fuel has good lubricating properties and when it enters the soil, it is quickly broken down by bacteria. The use of biodiesel significantly reduces emissions of greenhouse gases, hydrocarbons, carbon monoxide, soot and carcinogens; exhaust gas haze is reduced [53–59].

These indicators can have a positive effect on the service life of a diesel engine. However, there are disadvantages that need to be addressed: biodiesel increases the chemical wear of diesel engine parts because it is more aggressive than conventional diesel fuel [60–65].

The conducted analysis showed that the use of biological fuels and lubricants for mobile agricultural machines requires additional research to improve the reliability of elements and assemblies of their functional systems, taking into account the environment and operating mode.

The piston with a packet of piston rings and a cylinder are one of the most important kinematic nodes of an internal combustion engine. Caring for environmental protection, raising travel standards, lowering operating and production costs, and the requirement of unreliability force constant work on new solutions in the design, production and operation of internal combustion engines [66]. The cooperation of individual elements of the piston-cylinder group has a significant impact on the efficiency of the engine and its durability. Detailed knowledge of the phenomena of lubrication and wear occurring during the cooperation of the elements of the piston-cylinder group enables work on the improvement of the design of the piston-ring-cylinder unit [67]. Friction losses determine the mechanical efficiency of the engine. Reducing friction losses helps to reduce the amount of fuel consumed when performing the same work. In modern internal combustion engines, the piston and piston rings account for most of the frictional losses. The piston-cylinder assembly may account for even about 60% of the total mechanical losses in an internal combustion engine [68]. The tribological operation of the piston-cylinder unit has a significant impact on the efficiency and durability of the internal combustion engine. During

the operation of the internal combustion engine, the bottom of the piston is exposed to direct contact with the working medium of the internal combustion engine, located in the engine's working chamber. As a result of the combustion process, the temperature of the working medium can reach even 2000 °C. The inevitable effect of such a high temperature is heat transfer, which occurs mainly through transfer [69]. The heat exchange between the working medium and the bottom changes periodically. Taking into account the significant rotational speeds of the crankshaft of the internal combustion engine, the periods of changes are small [70].

An important problem in operational practice is the assessment of the technical condition of the engine, and thus the determination of the wear of the piston-rings-cylinder components (TPC) system [71]. The methods commonly used so far require partial disassembly of engine components to make the appropriate measurements. This group of methods includes the micrometer of engine components, as well as methods allowing the indirect determination of the degree of wear of the TPC system, e.g., compression pressure measurement. In this case, some components of the engine injection system must be dismantled. A separate group consists of methods that allow for continuous observation of the wear process of frictionally cooperating elements. The isotope methods used in this case, for example, are expensive and require specialist preparation, as well as instrumentation; therefore, they are not commonly used in technical diagnostics. The analysis of the piston-rings-cylinder system as a tribological system shows that the lubricant it contains may be an important source of information. Among all elements of the tribological system [72], engine oil undergoes the most intense physical and chemical changes during operation. This is due to the effect of the system on the oil [73]. When developing a new method of assessing wear of the TPC system, particular emphasis was placed on the possibility of its use by a wide range of vehicle users. Additionally, this method should not require interference with the tribological system or the vehicle's engine, and all measurements should be performed outside the vehicle. This approach required solving two fundamental problems: the choice of the method of assessing wear of the TPC system and the development of a methodology for testing the used engine oil. The necessary condition for assessing the wear of engine cylinder liners on the basis of changes in oil viscosity is the collection of the following information:

1. Kinematic viscosity at 100 °C- $\nu_{100}$  for fresh oil,
2. Kinematic viscosity at 100 °C- $\nu_{100}$  for used oil (in the time of its replacement),
3. Oil working time-vehicle mileage from the time of the last change.

The presented method allows us, with the accepted confidence level, to make an assessment for the 359M engine and engines of similar design. This dependence is not universal and its application to engines of a different type requires additional verification tests. However, the nature of the phenomena occurring in the engine oil and their dependence on the degree of wear of the TPC system suggest that the nature of the relationship will be similar. The differences will appear only in the values of the curve coefficients describing the relationship between consumption and the index  $C \nu_{100}$  [71].

The results of stand tests of the course of tribological wear of elements of compression ignition engine injection systems are presented. The authors presented a method of assessing the wear of the pumping sections of injection pumps. The results of the stand tests were given and the influence of the biofuel prepared on the basis of camelina oil methyl esters on the wear of the forcing sections was assessed [74].

In many tribological experiments to assess the thickness of the oil film, electrical methods, in particular resistance ones, are used [75]. However, the authors' research and the literature on triboelectric phenomena show that this is a wrong approach. During hydrodynamic friction, where the intensity of electric charge formation is negligible, one can indicate a correlation of the resistance in the friction zone with the thickness of the oil between the friction surfaces. However, in mixed or boundary friction, or even elasto-hydrodynamic friction, care should be taken when directly comparing the thickness of the oil layer with the resistance. The reason for this is the changing conductivity of the

oil film as a result of the formation and accumulation of electric charges in the oil. As it follows from Ohm's law, any change in the electrical voltage or current will be reflected in the resulting resistance. Therefore, more attention should be paid to the selection of an appropriate research technique to assess the thickness of the lubricating layer—to obtain relatively reliable information from the observation of the friction zone, many complex research methods should be used [76].

Tribological models [77] of cooperation of the piston-ring-piston-cylinder sleeve association illustrate the various conditions of cooperation of the abovementioned internal combustion engine coupling components. Traditional mechanical machining, i.e., boring and two-stage honing (preliminary and finishing on the plateau), does not ensure proper cooperation of the described tribological association. In the sensitive upper zone of the annular cylinder liner, boundary lubrication occurs with a very frequent break of the oil film, thus causing accelerated wear processes of the internal combustion engine components. Traditional machining does not allow for the production of a model topography of the surface layer because of technological limitations (irregular microcracks with sharp edges and poorly maintaining the oil film). Using modern technologies of ablative micro-machining of cheese, the constructor and technologist are able to very precisely design the appropriate topography of the surface layer of the cylinder liner and other elements of the association. The production of regular oil microcontrollers in the form of microchannels and cylindrical microcells allows the maintenance of an oil microfilm separating the cooperating elements of the association. Ablative laser micromachining offers great opportunities for the production of modified micro- and nanostructures in the surface layer in the sensitive zone (upper zone of the cylinder liner) through the interaction of laser plasma and high pressure. Fast-changing laser pulses with a repetition frequency from several to several dozen kHz force the laser ablation process, fragmentation of the structure and ultrafast phase transformations not achieved by other technologies. The results of preliminary tests indicate that thin amorphous (glassy) microlayers can be produced in the top layer—with very high technological values and very competitive with other modern technologies used in surface engineering. The laser modification processes not only qualitatively affect the structure, but also allow for the precise shaping of oil micro-reservoirs in sensitive areas. Hybrid technology, i.e., a combination of mechanical and laser processing, also creates great technological possibilities. In the first stage of the process, preliminary honing is performed, and in the second stage, micro-oil reservoirs are created and a finishing plateau is performed. Mechanical treatment is used to remove micro-flashes resulting from the technological process of ablative laser micro-machining. A significant advantage of this innovative technology is a very small heat-affected zone, which will probably have a minimal effect on the state of deformation of the sleeve and at the same time on its own stresses. From the technological point of view, the system of oil micro-reservoirs produced on the surface of the cylinder liner is equally important, as it has a decisive influence on the tribological processes [77].

Therefore, the work is based on research on the development of a methodology for assessing the tribotechnical properties of biofuels.

The aim of the work is to develop a method for assessing the consumption of materials of the cylinder-piston group of diesel engines in the biodiesel environment.

Taking as a working hypothesis that the reason for the accelerated wear of friction pair in the biofuel environment lies in the hydrogen saturation of the surfaces, we can reveal the mechanism of interaction of different structural materials during friction. It was assumed that the reason for such a situation is that oxide films appear on the surfaces of the samples and molecular hydrogen penetrates into the structure of the surface layers—this assumption is new in the article.

## 2. Materials and Methods

The development of this technique was based on the performed works related to the classical methods of experimental friction research [54,56,60,64,78,79]. To deal with the tasks, a systematic approach was used in wear resistance tests.

B70 biodiesel was used as biofuel, i.e., 70% mineral diesel oil and 30% rapeseed oil methyl esters. In terms of basic physicochemical parameters, this ratio corresponds to mineral diesel oil used in self-ignition tractor engines.

Experimental tribotechnical studies of the biofuels' influence on the behavior of various materials have shown that while using this type of fuel needs to be replaced, the materials of some parts of the cylinder-piston group are made from them.

To solve this problem, scientific research on a specially designed friction machine was conducted, as shown in Figure 1.

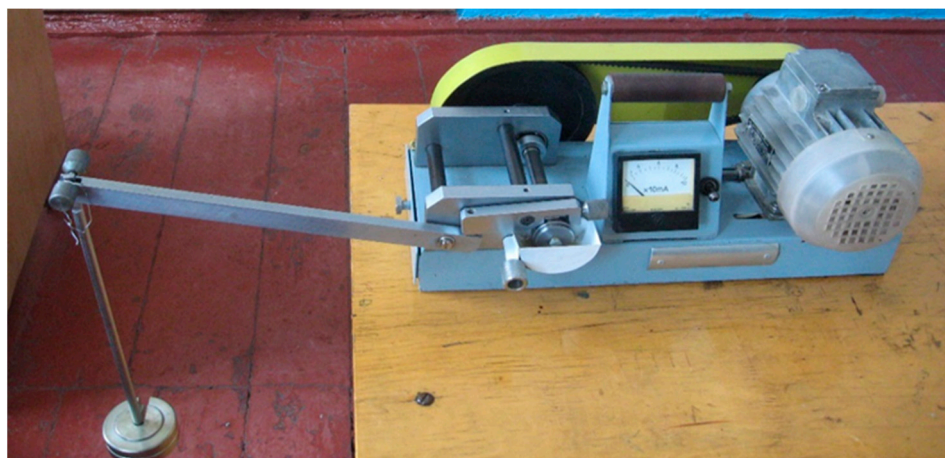


Figure 1. General view of the friction machine of the roller-pad system [own study].

Some basic materials that are used for producing the details of the cylinder-piston group were chosen as the objects of research. Characteristics of the materials are shown in Table 2.

Table 2. Parameters of the tested pad materials [own study].

Material	Chemical Composition, %								Hardness Rockwella, H, HRC
	C	Si	Mn	Cr	P	S	Ni	Cu	
Steel 45	0.42–0.50	0.17–0.37	0.50–0.80	–	0.035	0.04	–	–	58.0
Cast iron SCh 20	3.0–3.3	1.3–1.7	0.8–1.2	0.3	0.3	0.15	0.5	–	18.0
	Chemical Composition, %								
	Pb	Zn	Sn	Ti	Cu	Al	Si	Fe	
Bronze Br OCS 5-5-5	4.0–6.0	4.0–6.0	4.0–6.0	–	other				6.0
Aluminum A0	–	0.08	–	0.03	0.02	99.0	0.50	0.50	3.0

The sleeve was made of steel ShH15 (analogue of steel 1.3505) with a surface hardness of 60–62 HRC. The following materials were tested: bronze Br OCS 5-5-5 (analogue material 2.1097); gray cast iron SCh 20 (analogue GG20); steel 45 (analogue of steel 1.0503) (heat treated); and aluminum A0 (analogue ENAW-1100).

The evaluation of the efficiency of materials use on the friction machine was performed in accordance with the following parameters: ultimate load, area, volume and condition of the wear spot surface; critical specific load.

The procedure of the experiment included the following steps: the investigated friction samples were installed and fixed (before installation on the friction machine, the samples were polished and ground according to the conventional methods (GOST 23.210-80)). The roughness of the working surface was brought to Ra 0.16; the fuel was poured into the bath; the rig started and tests were performed without load for 1–3 min, then the load

on the friction pair was gradually increased until jamming caused by their grasp and the maximum load was recorded; after the load was removed and the studied samples were disassembled, the size of the wear spot of friction pairs materials was defined, and mineral fuel was replaced with biofuel; the friction unit was again formed and comparative studies were conducted according to the method explained above.

To conduct the experiment, the friction machine was improved and adjusted, and further calculations allowed us to develop a method of research.

Before conducting the experiment, it was necessary to calculate the rig parameters. To calculate the force acting on the sleeve without load, the distance from the center of the axes of the mounting arm that is acting on the clamping bar was measured, as shown in Figure 2.

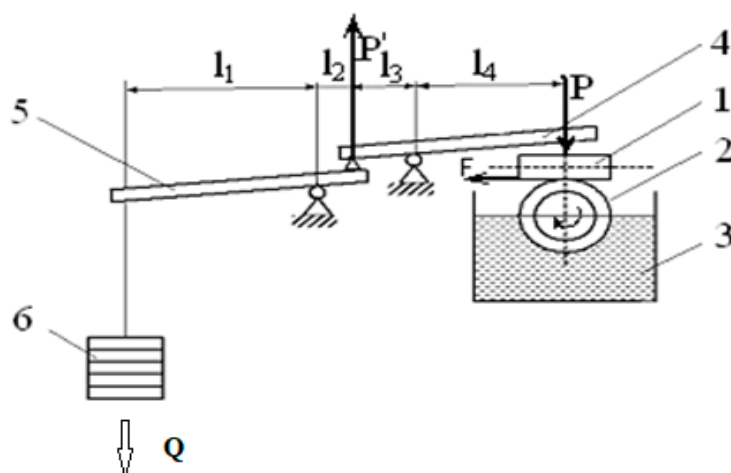


**Figure 2.** The scheme of loading of friction pairs [own study]: 1—sleeve; 2—roller; 3—lubricating environment; 4—clamping bar; 5—the lever; 6—load; symbols:  $l_1$ —the distance from the loading point to the axis of the lever attachment, m;  $l_2$ —the distance from the axis of lever the attachment to the point of its action on the clamping bar, m;  $l_3$ —the distance from the point of the lever action on the clamping bar to the axis of bar attachment, m;  $l_4$ —the distance from the axis of the clamping bar attachment to the point of application of the loading on the sleeve, m;  $P$ —the force acting on the sleeve, N;  $P'$ —the force acting on the clamping bar, N;  $F$ —the friction force, N;  $Q$ —the loading, N.

The tribotechnical tests were carried out on the developed friction machine using the Timken method. This installation enables the tribological process to be carried out under controlled conditions with the modeling of the speed, load and temperature modes of tribo-pairs, and also select the construction materials of the friction pair according to the shaft-sleeve or shaft-block scheme, as shown in Figure 2. This scheme allows modeling the operation of the cylinder-piston assembly according to the piston ring-sleeve scheme. This will shorten the test time compared to the actual operating conditions and will make it possible to predict the service life of tribo pairs when operating on alternative biodiesel fuels.

### 3. Results and Discussion

The relative sliding speed of the sleeve  $w$  was determined by Formula (1):

$$w = \pi \cdot D \cdot n; \quad (1)$$

where  $D$  is the diameter of the drive pulley, m; and  $n$  the engine speed, rpm.

As a result of calculations, the speed of sliding of the sleeve on the pad was received,  $w = 71.25 \text{ m} \cdot \text{min}^{-1}$ . The force  $P'$  acting on the clamping bar was found by Formula (2):

$$P' = \frac{Q \cdot l_1}{l_2}; \quad (2)$$

where  $P'$  is the force acting on the sleeve, N;  $Q$  the loading, N;  $l_1$  the distance from the loading point to the axis of the lever attachment, m; and  $l_2$  the distance from the axis of lever the attachment to the point of its action on the clamping bar, m.

The force acting on the sleeve  $P$  was calculated by Formula (3):

$$P = \frac{P' \cdot l_3}{l_4} = 2P'; \quad (3)$$

where  $P'$  is the force acting on the sleeve, N;  $l_3$  the distance from the point of the lever action on the clamping bar to the axis of bar attachment, m; and  $l_4$  the distance from the axis of the clamping bar attachment to the point of application of the loading on the sleeve, m.

After carrying out the necessary calculations, it was found that at the point of contact the force is  $P = 613.5$  N. Knowing the force at contact, you can calculate the friction force  $F$ ; because the friction occurs on a homogeneous material steel ShH15, the friction coefficient  $\mu$  will be equal to (4):

$$\mu = \frac{F}{P} \quad (4)$$

For the dependencies presented in this way, Table 3 summarizes the influence of the load on the friction force  $F$  and the force on the working pair  $P$  at dry friction and the friction coefficient.

**Table 3.** The influence of loading on the friction force  $F$  and the force on the working  $P$  pair at dry friction [own study].

Sample	Friction Force $F$ , N	The Force on Working Pair $P$ , N	Coefficients of Friction $\mu$
Without load	8	21.05	0.38
1 load *	16	42.10	0.37
2 loads	24	61.35	0.39

\* weight of one load—480 g.

According to the obtained data, a graph of the dependence of the friction force  $F$  on the loading  $Z$  was built, as shown in Figure 3.

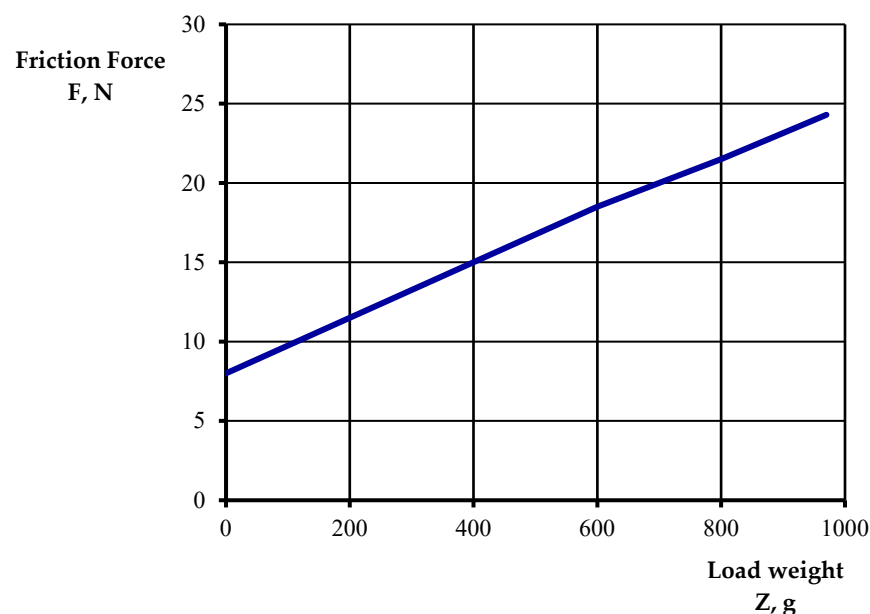


**Figure 3.** Graph of the dependence of friction  $F$ , N on the loading  $Z$ , g [own study].

After calibrating the scale of the ammeter, which shows the load of the engine depending on the amount of load on the shoulder, the following experiment, which used

loads weighing  $Z$ : 50 g, 100 g, 200 g, 480 g, was conducted. The obtained data are shown in Table 4.

**Table 4.** Ammeter  $\Theta$  calibration results [own study].

Indicator	Value				
Weight of the load $Z$ , g	0	50	100	200	480
Current (ammeter reading) $\Theta$ , A	3.25	3.5	3.75	4.15	4.95

According to the obtained data, a graph of the dependence of current  $\Theta$  on the load weight  $Z$  was built, as shown in Figure 4.

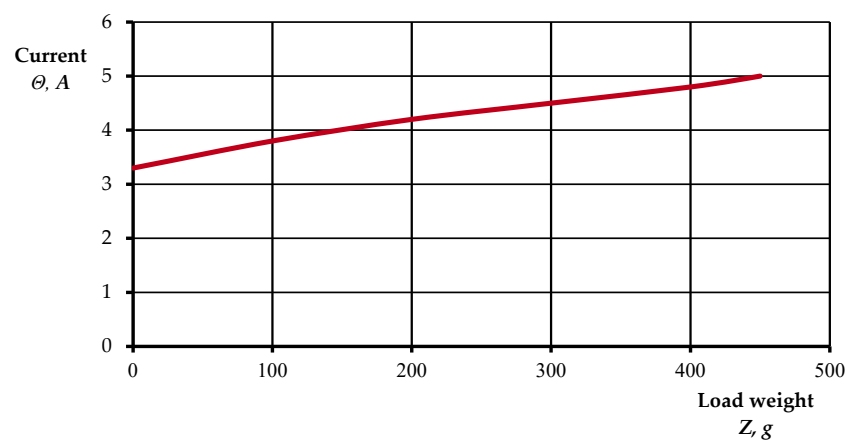


**Figure 4.** Graph of the dependence of current  $\Theta$  on the mass of the load  $Z$  [own study].

The analysis of the conducted research has allowed us:

- To substantiate a technique of laboratory research;
- To make a choice of laboratory equipment for tribotechnical research;
- To carry out the comparative description of biofuel influence on tribological properties of the materials of cylinder-piston group of diesel engines.

Tests for the wear of various materials were performed on the rig of the system roller-sleeve, which was improved and the roller was replaced by a pad for the convenience of worn material measuring, as shown in Figure 5.

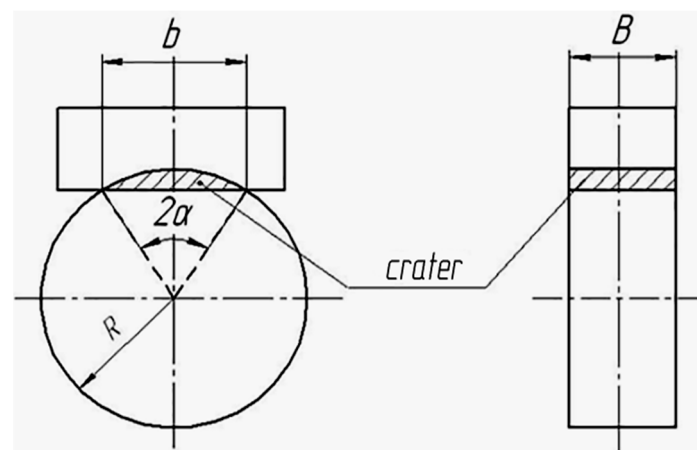


**Figure 5.** Parameters of the crater wear: symbols:  $b$ —width, m;  $B$ —length, m;  $R$ —radius, m; [own study].

The block, which is a sample of the square cross-section, was loaded with a force of  $P = 61.35$  N. The sleeve was made of steel ShH15 with a diameter of 30 mm. The relative sliding speed of the samples was  $w = 71.25$  m·min<sup>-1</sup>.

The friction force  $F$  in the contact zone was determined by the power consumption of the motor, in accordance with the preliminary calibration of the microammeter.

Important information about the wear mechanism was provided by the analysis of wear products—wear spots on the pad. For this purpose, the optical method of microscopic observations and measurements of the wear groove profile was used. The structure and measurements of crater wears were examined using an optical microscope (according to the method of measuring Brinell hardness), as shown in Figure 5.

Volumetric wear of tribounits  $V$  was determined by the Formula (5):

$$V = S \cdot B; \quad (5)$$

where  $B$  is the length of the pad crater, mm; and  $S$  is the area of the worn material, mm<sup>2</sup> (6):

$$S = \frac{\pi \cdot R^2 \cdot 2\alpha}{360^\circ} - \frac{R}{2} \cdot \sin 2\alpha. \quad (6)$$

For the convenience of calculating the area of worn material, using Formula (6), we received a calibration graph—Figure 6 of the dependence of the worn material area  $S$  on the length of the crater  $B$ .

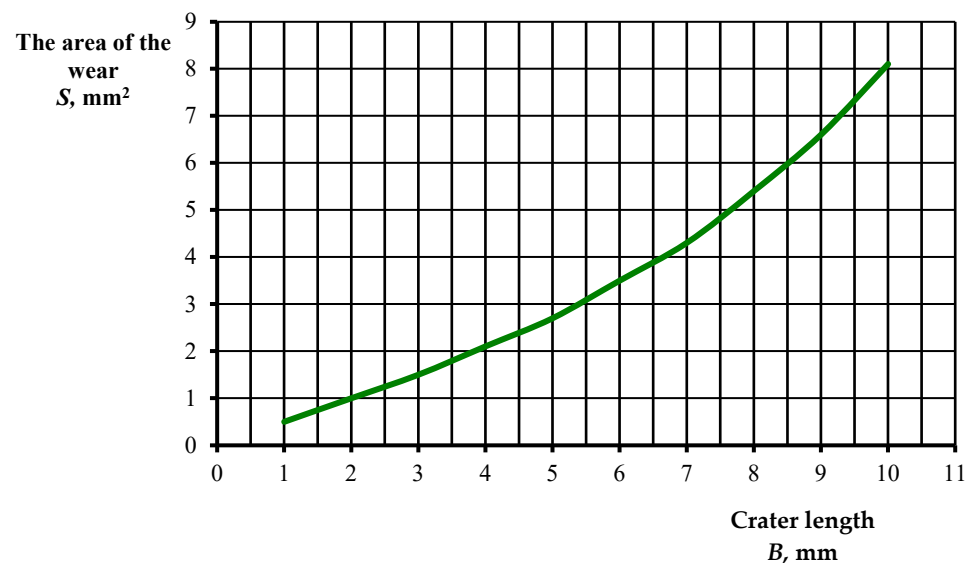


**Figure 6.** Calibration graph of the dependence of the worn material area  $S$  on the length of the crater  $B$  [own study].

Measurements of wear and friction force were performed every 75 m on the friction path E for 1 min. The width of the crater  $b$  of the sample (pads) when the pads wear on the sleeve was measured and followed by conversion to the volume of worn material  $V$ , wear intensity  $I$  and wear coefficient  $K_u$ . Experimental data are shown in Table 5.

Volumetric wear  $V$  of different materials under loading  $P = 61.35$  N and the relative sliding speed of the samples  $w = 71.25$  m·min<sup>-1</sup> in the biofuel environment are shown in Figure 7. As can be seen from these dependences, ferrous metals, steels and cast irons have much less bulk wear than aluminum and copper alloys.

**Table 5.** Experimental data on the wear of materials in the biofuel environment [own study].

Material	B, mm	Friction Path E, m													
		75		150		225		300		375		450		525	
		Current (Ammeter Reading) and the Width of the Crater													
		Θ, A	b mm	Θ, A	b mm	Θ, A	b mm	Θ, A	b mm	Θ, A	b mm	Θ, A	b mm	Θ, A	b mm
Bronze Br OCS 5-5-5	7.8	2.5	2	2.6	2.4	2.8	2.6	2.0	2.7	1.5	2.7	1.7	2.7	1.7	2.8
Cast iron SCh 20	6.7	2	0.8	2	1	2	1.1	2	1.2	2	1.3	2	1.4	2	1.5
Steel 45	7.0	3	0.5	2.9	0.6	2.8	0.7	2.9	0.8	2.9	0.85	2.9	0.9	2.9	1.0
Aluminium A0	8.0	2	2.2	2	2.8	2	3.1	2	3.4	2	3.6	2	3.7	2	3.8

The results of wear of the metal volume V depending on the friction path E are shown in Table 6.

**Table 6.** Wear of material volume V depending on the friction path E [own study].

Material	Friction Path E, m							
	75	150	225	300	375	450	525	
	Consumption of the Volume of the Material V, mm <sup>3</sup>							
Bronze Br OCS 5-5-5	7.57	9.36	10.3	11.2	11.7	11.9	12.1	
Cast iron SCh 20	2.68	3.4	3.8	4.02	4.36	4.7	5.0	
Steel 45	1.30	2.0	2.4	2.8	3.15	3.3	3.4	
Aluminium A0	11.5	14.7	16.0	17.5	18.5	19.5	20.3	

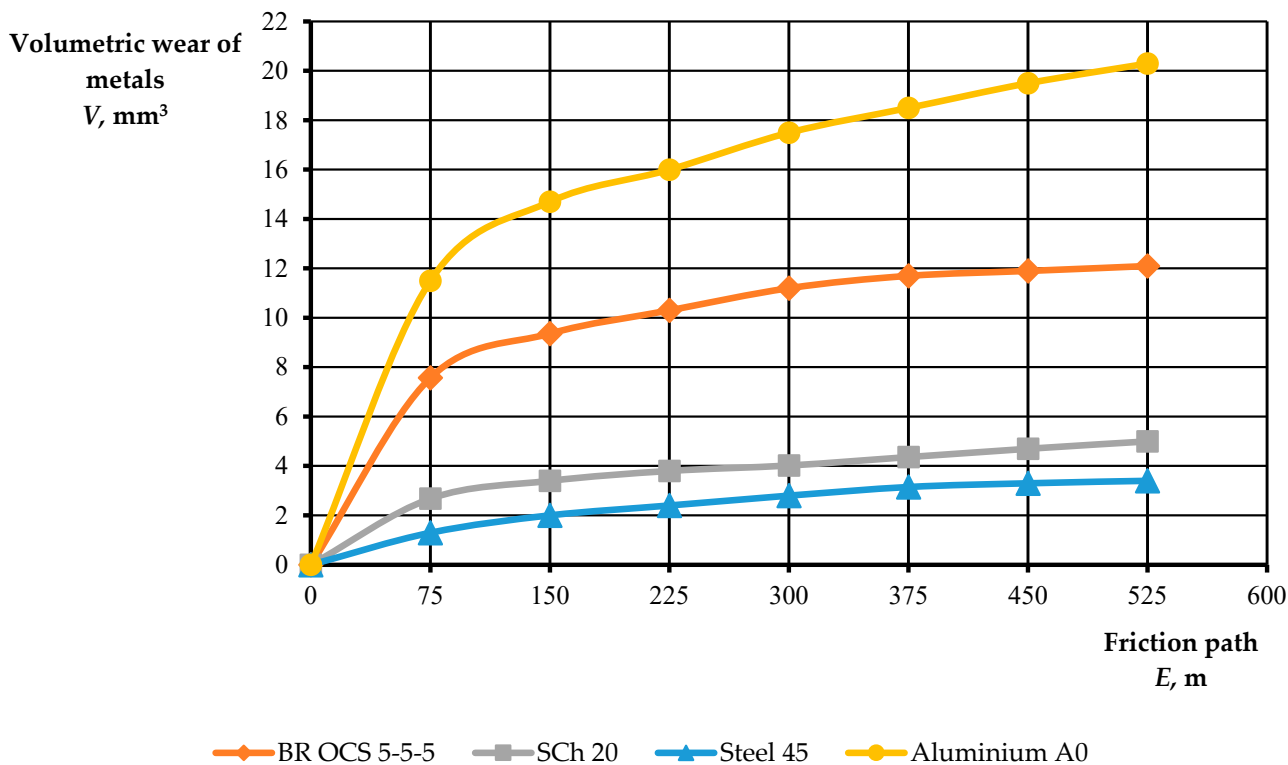


**Figure 7.** Dependence of volumetric wear V of metals on the path of relative samples movement (friction path) E in the biofuel environment [own study].

It follows from Figure 7 that the volumetric wear  $V$  curves obey the parabolic law and are described by the following empirical dependences: for bronze Br OCS 5-5-5 volumetric wear is described by Equation (7):

$$V = -0.000001 \cdot E^2 + 0.025 \cdot E + 6.225 \quad (7)$$

For steel ShH15 volumetric wear  $V$  is described by Equation (8):

$$V = -0.0000018 \cdot E^2 + 0.032 \cdot E + 2.85 \quad (8)$$

where  $E$  is the friction path, m.

According to the volumetric wear, the wear intensity  $I$  for different materials in the biofuel environment was calculated by Formula (9):

$$I = \frac{V}{T} \quad (9)$$

Data on the wear intensity are given in Table 7.

**Table 7.** The wear intensity  $I$  of the samples in the biofuel environment [own study].

Material	Experiment Length $t$ , min						
	1	2	3	4	5	6	7
	Wear Intensity $I$ , $\text{mm}^3 \cdot \text{min}^{-1}$						
Bronze BR OCS 5-5-5	7.57	4.68	3.43	2.8	2.34	1.98	1.73
Cast iron SCh 20	2.68	1.7	1.26	1.01	0.87	0.78	0.71
Steel 45	1.3	1.0	0.8	0.7	0.63	0.55	0.49
Aluminum A0	11.5	7.35	5.3	4.38	3.7	3.25	2.9

The dependences of the wear intensity  $I$  of the materials of the parts of the cylinder-piston group in the biofuel environment are shown in Figure 8.

Based on these dependencies, the wear intensity  $I$  is maximum in the initial period and stabilizes after 400 m of friction path  $E$ . Since these materials can be used in different friction pairs, at different speed and force parameters, the dependences of the wear coefficients of these test materials in the biofuel environment were obtained.

The wear coefficient was determined by the dependence (10):

$$K_U = \frac{F_U \cdot B}{P \cdot E} \quad (10)$$

where  $F_U$  is the cross-sectional area of the sample wear,  $\text{m}^2$ ;  $B$  is the width of the sample, m;  $P$  is the loading reaction of the friction unit, N; and  $E$  is friction path, m.

Therefore, the wear coefficient is a generalized indicator of the power, design and speed parameters of the tribounits parts that are worn. It allows us to determine the resistance of materials to wear in different environments.

The friction path was calculated by the rotation frequency of the roller and its diameter. The loading response was determined by recalculating the system of levers of the friction machine and checking with a dynamometer. The wear coefficients of different materials in the biofuel environment are shown in Table 8.

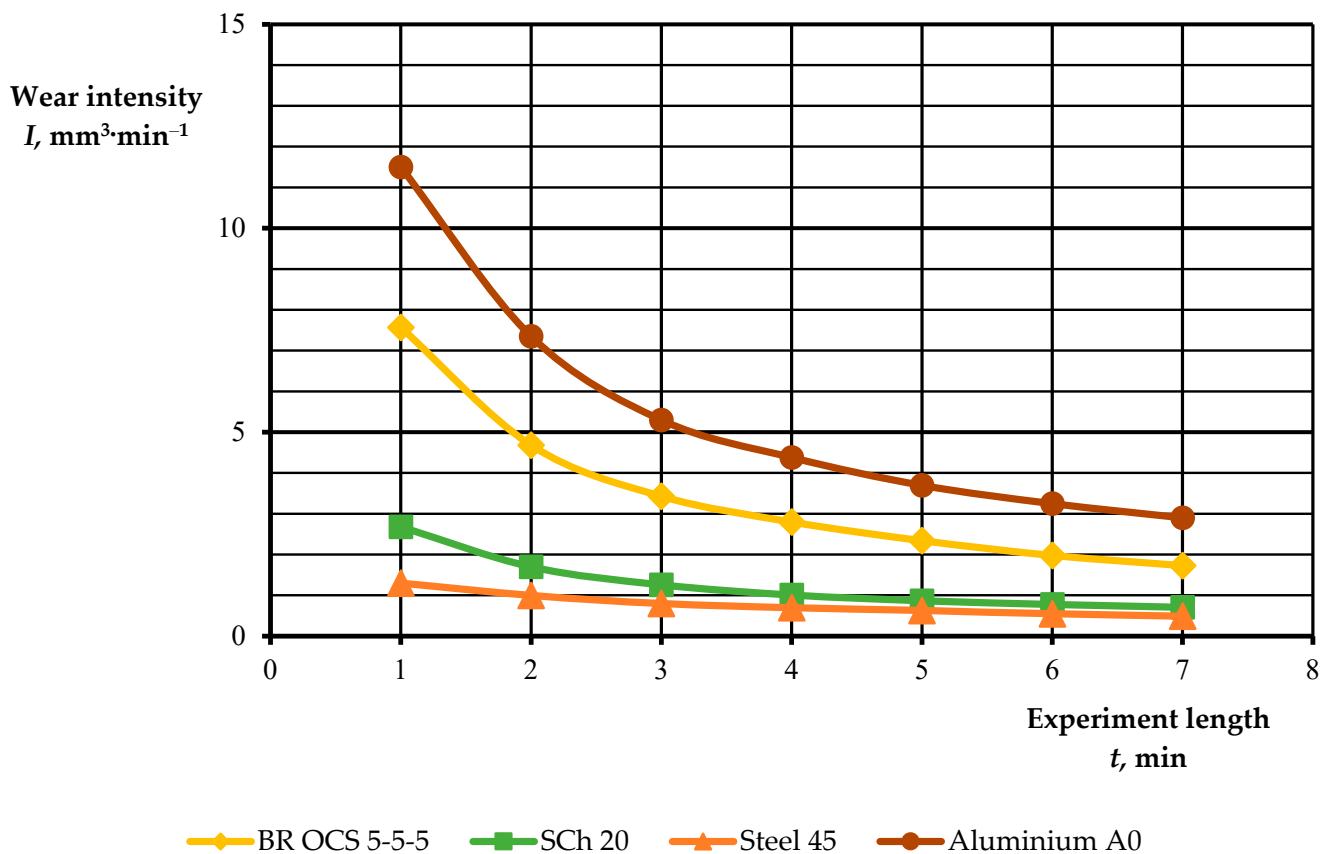


**Figure 8.** The wear intensity  $I$  of the materials of the parts of the cylinder-piston group in the biofuel environment [own study].

**Table 8.** Wear coefficients of materials  $K_U$  in the biofuel environment [own study].

Material	Friction Path E, m						
	75	150	220	290	360	430	500
	Wear Coefficients $K_U, \text{mm}^2 \cdot \text{N}^{-1}$						
Aluminum A0	0.250	0.168	0.122	0.098	0.082	0.072	0.065
Bronze	0.165	0.102	0.076	0.066	0.053	0.045	0.039
BR OCS 5-5-5	0.058	0.036	0.027	0.023	0.020	0.018	0.016
Cast iron SCh 20	0.046	0.027	0.019	0.016	0.014	0.013	0.011
Steel 45							

The change in wear coefficients  $K_U$  of different materials under loading  $P = 61.35 \text{ N}$  and the relative sliding speed of the samples  $w = 71.25 \text{ m/min}$  in the biofuel environment at wear are shown in Figure 9.

Figure 9 shows that the stabilization of wear coefficients in ferrous metals occurs after 300 m on the friction path, and in non-ferrous metals after 500 m on the friction path. Stabilization of the wear coefficient characterizes the period of running-in of the coupling parts, and the magnitude of the fall—the operation time of the allowable wear.

Based on the literature [80], it should be noted that hydrogen wear causes wear of the material in friction contacts if the conditions for the formation of atomic or ionic hydrogen and its adsorption by the surface are present on the surface of the metal forming the contact. Nuclear or ionic hydrogen in the frictional contact is formed, inter alia, during thermal decomposition of the lubricant, in the process of electrochemical corrosion and as a result of cathode reactions and thermal dissociation of molecular hydrogen. Nuclear hydrogen,

apart from penetrating into the material, can reduce the oxides on the surface, which causes an increase in the coefficient of friction and promotes the formation of adhesive tacking and wear by oxidation and removal of corrosion products. Hydrogen entering the metal can cause many types of damage, generally referred to as hydrogen damage. The main factors influencing hydrogen damage are material, stresses and medium. The prevention of hydrogen damage consists of the correct selection of materials, the process of their production and the design features of the element. Inhibitors and treatments are also used to reduce the hydrogen concentration in the material.

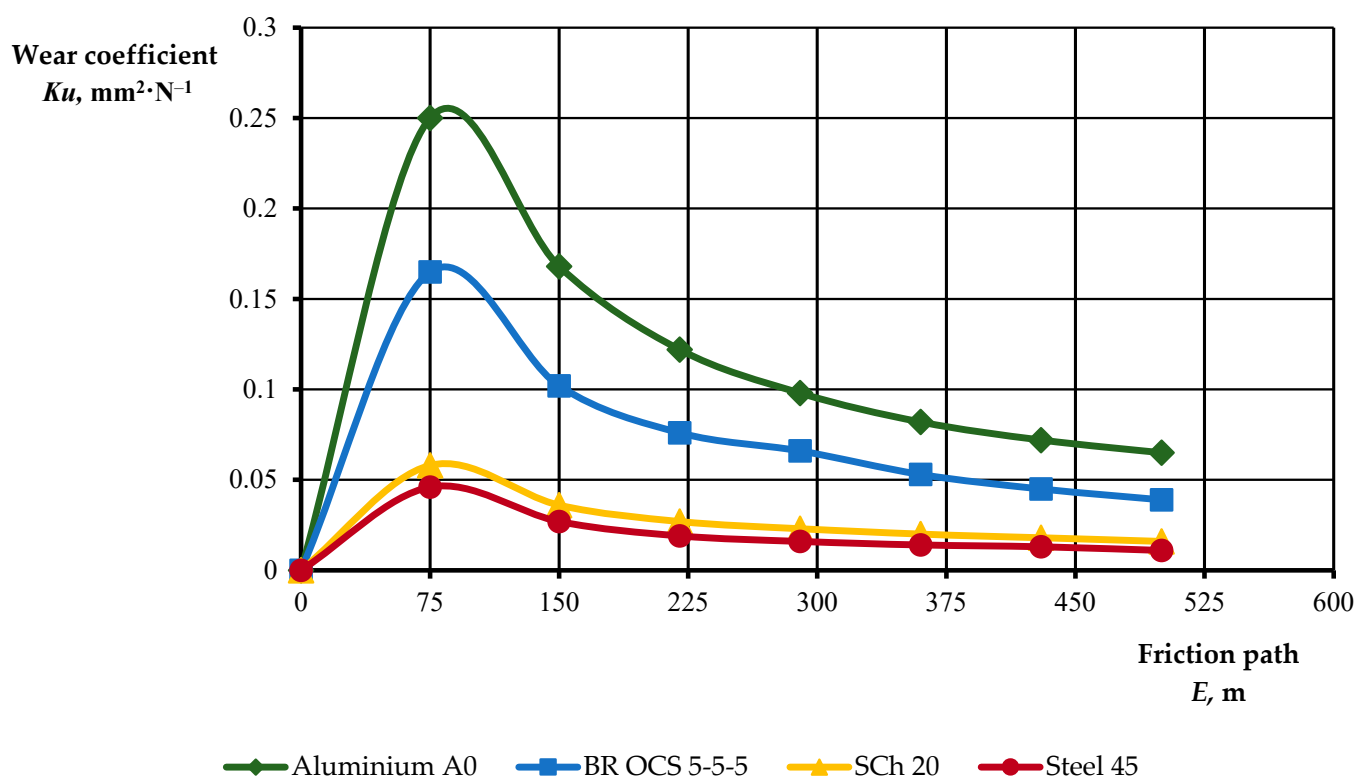


**Figure 9.** Change in the wear coefficients  $K_u$  of various materials in the biofuel environment at wear [own study].

The association demonstrated the hypothesis that the presence of large amounts of hydrogen in biofuels allows for an intensive formation of oxide films on the metal surface, which reduces the consumption of materials.

Hydrogen consumption is caused by the adsorption of hydrogen on the friction surface and its diffusion into the surface layer. Hydrogen at a certain concentration and with high diffusion capacity dissolves in practically all metals (except gold and mercury), causing a change in their physical, mechanical and operational properties and, as a consequence, premature wear. During the diffusion of hydrogen into the subsurface layer and the simultaneous large deformation of the surface material, hydrogen fills the voids in the defective structure. The cyclical formation of a moving wave of stresses (tension-compression) intensifies the saturation with hydrogen of the surface volumes of the material deformed by friction. As a result of these physical processes, the structure of the surface material is thinned. Retention of hydrogen in the “traps” present and formed in the friction process leads with time to an increase in the amount of hydrogen in the surface layers and, consequently, to a significant increase in internal stresses and a decrease in their wear resistance [81].

Hydrogen that has penetrated into steel significantly changes its mechanical and operational properties. The degree of this change depends on the chemical composition of the steel, microstructure, degree of contamination, number, type and distribution of

nonmetallic inclusions, as well as the type of thermal and mechanical treatment (plastic deformation) applied to it. Hydrogenation has the greatest impact on its strength and plastic properties (elongation and narrowing), the latter strongly decreasing with the increasing hydrogen content in the metal, contributing to the so-called phenomena of delayed cracking and stress—sulphide cracking. So far, it is believed that the occurring hydrogen embrittlement of steel depends not only on the amount of hydrogen adsorbed by the metal, but also on the state of stress—the occurrence of tensile stresses. The influence of steel deformation on the brittle fracture occurrence has not been taken into account so far. Until now, there is no clear answer to the question of which of these factors, namely the level of stress or deformation, and to what extent, determines the occurrence of hydrogen embrittlement. The analysis of the preliminary research on hydrogen embrittlement of both Armco iron and AISI 1095 high-strength steel shows [82] that their brittleness shows a strong dependence on the method of inducing plastic deformation in metals. Under the influence of dynamic but slowly increasing plastic deformation, the brittleness of metals increases [83].

The reduction of hydrogen penetration into the metal can be achieved by modifying the chemical composition of construction materials—steel [84]. The addition of nickel, platinum or cobalt significantly reduces the sorption of hydrogen in carbon steel. Lowering the hydrogenation of steel is also favored by the addition of chromium in the amount of  $0.2 \div 0.7\%$ , depending on the amount of molybdenum in the chemical composition of the steel, and the addition of more than  $0.02\%$  of gold or copper [84]. The process of hydrogen penetration into metals is also significantly reduced as a result of modifying their surface layers. Modification of metal surfaces inhibits the penetration of hydrogen into their modified surfaces (the so-called surface effect) and hinders the transport of hydrogen to the base of the metal proper (transport effect) [85]. Both the electrolytically deposited copper on the steel surface and the electrolytically or electrolytically generated nickel layer reduce the hydrogen permeation [86]. Anodic cadmium and zinc surface coatings, commonly used to protect steel against corrosion, also reduce the rate of hydrogen diffusion in these materials. The most effective in terms of reducing the rate of corrosion of steel and alloys and hydrogen penetration are Zn-Ni-Cd coatings obtained from alkaline sulphate baths under constant potential conditions [86]. Surface layers obtained in various nitriding processes are characterized by favorable mechanical properties, including those increasing the resistance of metals to corrosion, as well as to the damaging effect of hydrogen [85,87,88].

At room temperature, the hydrogen atoms are absorbed by the metal structure and scattered by its grains. Hydrogen can be stored in atomic or molecular form. Regardless of the form, atoms and molecules will fuse to form tiny bubbles at the boundaries between the grains of the metal. These bubbles build up pressure to levels where metals lose their plasticity, resulting in tiny cracks. The susceptibility of materials to hydrogen embrittlement depends on the characteristics of their microstructure and the presence of defects. Scientists initiated the MULTIHY (multiscale modeling of hydrogen embrittlement) project, funded by the EU, to develop tools to assess hydrogen transport in high-strength alloys with complex microstructures and to better understand the phenomenon of hydrogen embrittlement. Researchers identified links between the influence of micro- or nano-scale structural aspects and macro-measurable factors of exposure to hydrogen embrittlement. Analytical techniques, physical tests and data from actual production installations were used to develop a multi-scale modeling structure for hydrogen transport from the atomic level to the component level [89].

In the work [90], the formation of a copper layer from a grease filled with a copper complex characteristic of a copper alloy (a reaction product of copper hydroxide and caprolactam) is explained by the tribochemical changes taking place in the frictional contact area. The probable course of this process is as follows: in the process of tribochemical transformations a radical is formed and atomic hydrogen is released [91].

Hydrogen is also a disadvantageous gas in cast iron, which may reduce plastic properties and may cause punctures [92].

The reaction with hydrogen in the solid state is better investigated in relation to plastically treated aluminum alloys and includes the phenomenon of stress corrosion cracking, in which, under mechanical load and under the influence of a corrosive medium, a simultaneous anodic dissolution reaction and cathodic loss of elasticity under the influence of hydrogen and the environmentally assisted cracking (EAC) phenomenon, which describes the sheer loss of flexibility under moist air conditions without dissolving the material, may occur. In addition, the effect of dry hydrogen gas on the mechanical properties of aluminum and its alloys has already been studied by various groups and classified as irrelevant. It is supposed that the reason may be the protective effect of a thin oxidation layer on aluminum, which inhibits the processes of energetically unfavorable decay and accumulation of hydrogen molecules. The degradation of the mechanical properties of aluminum materials that is due to the presence of hydrogen is most often attributed to the accumulation of hydrogen in “traps” such as grain boundaries, expulsions, dislocations and vacancies—and leads to a local reduction in ductility. Known mechanisms are “hydrogen-enhanced localized plasticity (HELP), hydrogen-enhanced decohesion (HEDE) and absorption-induced dislocation emission (AIDE)”. Thus, the susceptibility to a loss of elasticity caused by the presence of hydrogen can be correlated, inter alia, by the microstructure present. For wrought aluminum alloys, susceptibility to both stress corrosion and EAC has already been observed. The dominance of loss of elasticity caused by the presence of hydrogen in the case of stress corrosion cracking has not yet been unequivocally explained, but during the EAC test, a clear correlation was found between the crack expansion rate and the relative humidity, which determines the amount of hydrogen discharged [93].

Structural and tool steels show the lowest consumption in the biofuel environment. Aluminum and copper alloys have the lowest wear resistance in the biofuel environment. In ferrous metals, the run-in period is within a radius of 300 m from the relative slip of the parts. Nonferrous metals and alloys stabilize the wear properties only after a relative displacement of 500 m (friction path).

The intensity of this type of consumption, according to our assumption, can be controlled by changing the concentration of methanol in biodiesel. This is one of the most important conclusions from the research, as reducing the concentration of methanol in biodiesel will prevent hydrogen permeation into the surface layers of construction materials, which will reduce hydrogen consumption—based on our hypothesis.

Moving from mobile equipment to a methanol-based biofuel requires a careful approach to fuel material selection and other mobile equipment engine systems. The results of the research are presented in the histogram in Figure 10; by analyzing it, it can be concluded that the materials most sensitive to biofuels are aluminum A0 and bronze Br.

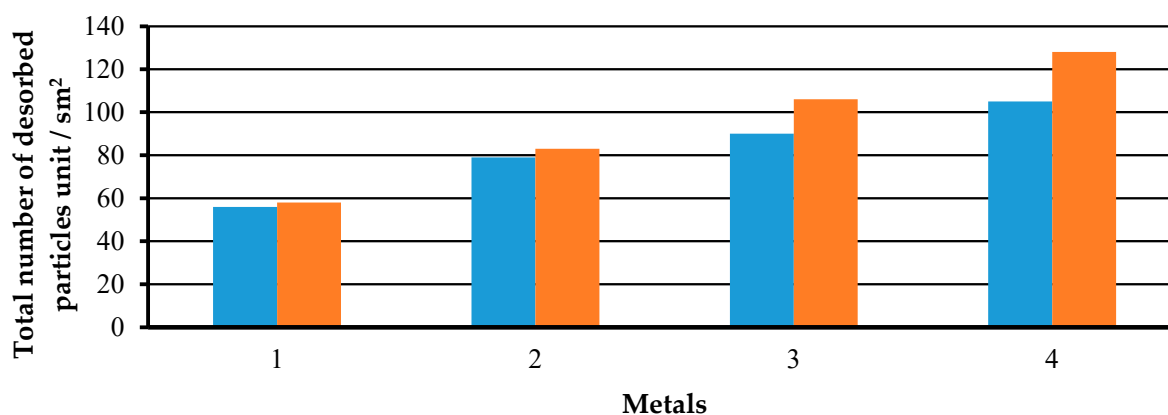


**Figure 10.** Root mean square (RMS) and arithmetic mean values of the total number of desorbed particles per unit of the sample surface during desorption on different metals [own study]: 1—steel 45; 2—cast iron SCh 20; 3—bronze Br OCS -5-5-5; 4—aluminum A0.

This gives a reason to recommend avoiding the use of these materials for direct contact with biodiesel. In addition, it can be argued that in the biodiesel fuel environment, hydrogen wear of friction pairs will be observed.

Various types of mercaptans are found in oil and its products, including fuels and lubricants, as well as in the other organic oils derived from biological raw materials. The scientific papers described the mercaptans impact on the anti-wear properties of fuels for engines and stated that the complete absence of mercaptans in fuels that is due to hydrotreating, impairs their anti-wear properties and leads to negative consequences.

When adapting engines to biofuel, parts made of plastic and rubber must be replaced with materials that are inert to the acidic environment.

Thermo-oxidative stability of fuel at elevated temperatures determines its tendency to deposit on engine parts and injectors. This important operating parameter of commercial diesel fuels is still little-studied, and research of thermal oxidative stability of biofuels is practically not carried out.

To improve the technical and economic performance of biodiesel, it is necessary to intensify the processes of injection, mixing and combustion. Heating to a temperature of 70–80 °C can have a positive effect on these processes, which will lead to the improvement of its physicochemical parameters. Subsequently, increasing the injection pressure will reduce the diameter of the spray droplets, and the intensification of air turbulence will improve the processes of evaporation and mixing.

To predict the operation time of the cylinder-piston group couplings, in this case the “cylinder liner and piston rings”, it is necessary to know how the coupling parts will behave during operation, as well as what kind of wear will take place. This is possible in the presence of a general indicator of speed, force and design parameters of conjugations, which is the wear coefficient obtained by us in the process of experiments.

The aim is to establish analytical and experimental dependences for predicting the operation time up to conjugation failure caused by the wear coefficient. Therefore, knowing the time to failure, you can predict the operation time of the unit as a whole.

Since the resource of the unit is determined by the wear of the main connections, a slightly different approach is possible when predicting their operation time. Knowing the value of the maximum wear  $U_{lim}$  of individual connections according to the calculation schemes, it is possible to determine the maximum operating time of individual connections of the unit  $T$ .

Numerical values of the wear coefficient  $K_U$  during normal wear can be obtained by Formula (10), then the friction path  $E$  will be equal to (11):

$$E = \frac{F_U \cdot b}{P \cdot K_U} \quad (11)$$

where  $P$  is the conjugate force, N;  $K_U$  is the wear coefficient in a stable period,  $m^2 \cdot N^{-1}$ ;  $F_U$  is the longitudinal wear section,  $m^2$ ; and  $b$  is the width of contact surfaces, m (12):

$$b = \pi \cdot D_c \quad (12)$$

where  $D_c$  is the diameter of the cylinder, m.

The friction path  $E$  can be calculated using the design parameters of the engine (13):

$$E = n \cdot T \cdot L \quad (13)$$

where  $n$  is the number of cycles, rpm;  $L$  the piston stroke length, m; and  $T$  the conjugation resource, moto-hour.

From here we find the resource of tribounit (14):

$$T = \frac{E}{n \cdot L} \quad (14)$$

Based on Formula (11), the resource can be defined as follows (15):

$$T = \frac{F_U \cdot b}{P \cdot K_U \cdot n \cdot L} \quad (15)$$

Based on the Formula (12), the expression for finding the resource takes the following form (16):

$$T = \frac{F_U \cdot \pi \cdot D_c}{P \cdot K_U \cdot n \cdot L} \quad (16)$$

where  $F_U$  is the longitudinal wear section,  $F_U = L \cdot U_{\text{lim}}$ .

Figure 11 shows the calculation scheme for estimating the wear limit in the friction pair piston ring-cylinder liner.

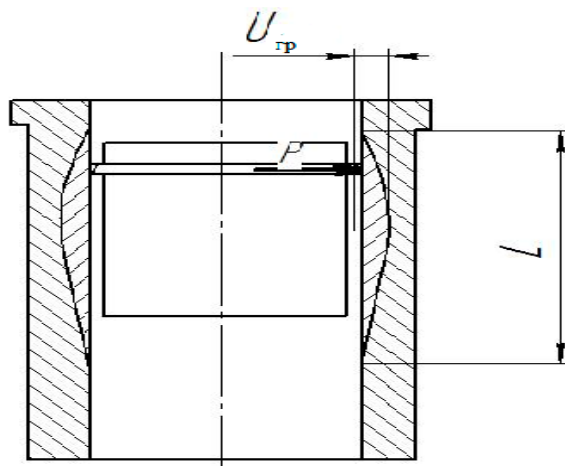


**Figure 11.** Calculation scheme for estimating the wear limit in the tribounit piston ring-cylinder liner [own study].

With known values of the wear coefficient  $K_U$ , operating conditions ( $P, n, L$ ) and wear limit  $U_{\text{lim}}$ , the resource in the tribounit piston ring-cylinder liner  $T$  is found by Formula (17):

$$T = \frac{U_{sp}^2 \cdot \pi \cdot D_{\mu}}{P \cdot K_U \cdot n \cdot L}; \quad (17)$$

Therefore, the obtained experimental dependences of the wear coefficients on the example of the tribounit cylinder liner-piston ring can be used to predict the resource while working in specific engine operating conditions and the environment as a whole.

The progressive exploitation of nonrenewable resources such as coal, oil and gas leads to the overconsumption of these resources and the depletion of stocks [94]. The beginning of the industrial era based on energy-intensive systems has resulted in an increase in energy demand. For the past few years, the world has seen an increased interest in the production of fuels from organic sources [95]. This is due to the overlapping of several factors: high oil prices, the desire of individual countries for energy sovereignty, the fight against global warming, and limited resources of non-renewable raw materials. To meet the challenges faced by the energy sector and to meet the requirements of environmental protection, the development of renewable energy sources is necessary [96–98]. Biofuels are all fuels produced from biomass. Biomass is considered to be any biodegradable animal and plant matter and products of their metabolism [8]. Biofuels can be gaseous, solid or liquid. The representative of the first group is biogas obtained by anaerobic digestion [99–101]. Liquid biofuels are mainly bioethanol (ethyl alcohol produced from plants in fermentation and distillation processes) and biodiesel (chemically processed oil). Solid biofuels are processed and unprocessed biomass, as well as the biodegradable fraction of municipal waste. All of these biofuels are used in the heating and power sector [102–104].

The development of biofuels in the world is aimed at developing profitable methods of obtaining them, while minimizing the negative impact on the environment and ensuring availability. The development of biofuel production is a new area of economic activity and a key element in the development of the bioeconomy, which belongs to the area of smart specialization. Its essence lies in the innovative use and management of renewable biological resources to create new types of products and production techniques, while maintaining the requirements of sustainable development [11]. Currently, the aim is to promote second and third generation biofuels; research and development works are underway to develop innovative technologies for obtaining those biofuels that do not compete with crops for food purposes and do not reduce biodiversity, thanks to which the negative aspects of introducing biofuels, despite increasing their share in the total pool of fuels, can be minimized. Due to the insufficient amount of raw materials and competition with crops for food purposes, the possibilities of producing first generation biofuels are limited [2].

Unfavorable changes in the Earth's climate, concerns about the energy future and the need to protect natural resources become the reasons to search for alternative solutions [105,106]. In addition, regulations and legal provisions oblige EU countries to reduce emissions of pollutants into the atmosphere (reduction of greenhouse gas emissions from transport by 60% by 2050, compared to 1990), and therefore increase the share of biodiesel in total use [107]. The European Union signed the 20/20/20 decree, which obliged the governments of all countries to increase energy efficiency by 20%, reduce greenhouse gas emissions by 20% and increase by 20% the total amount of energy produced from renewable sources by 2020 [108,109].

#### 4. Conclusions

Experimental tribotechnical studies of the influence of biofuels on the behavior of the sleeve, which was made of ShH15 steel, were carried out in relation to some parts of the cylinder-piston group: bronze Br OCS 5-5-5, gray cast iron SCh 20, Steel 45 and aluminum A0.

The assessment of the effectiveness of the use of materials on the friction machine was carried out in accordance with the following parameters: limit load, surface, volume and surface condition of the wear site and critical specific load.

The volumetric consumption and the consumption intensity of various materials under appropriate load and the relative sliding speed of the samples in the biofuel environment determine the relationship for ferrous metals; steels and cast irons consume much less than aluminum and copper alloys.

The change in the wear coefficients of various materials under load and the relative sliding speed of the samples in the biofuel environment with the consumption of the materials of the cylinder-piston assembly are determined by the dependence for the stabilization of the wear coefficients in ferrous metals after a 300 m friction path, and in nonferrous metals after a 500 m friction path.

According to the assumption, the consumption intensity can be controlled by changing the concentration of methanol in the biodiesel, as reducing the concentration of methanol in the biodiesel will prevent the hydrogen permeation into surface layers of building materials, which will reduce hydrogen consumption—our hypothesis follows.

The main factors influencing hydrogen damage are material, stress and medium. Prevention of hydrogen damage consists of the correct selection of materials, the process of their production and the design features of the element.

The presence of hydrogen in metals and alloys adversely affects their physical and mechanical properties, which is manifested, among other ways, by reduced mechanical strength and increased brittleness.

It is necessary to develop a material index enabling the assessment and classification of metals and alloys in terms of their susceptibility to hydrogen absorption.

On the basis of this index, it would be possible to correctly select metals for structural elements operating under the influence of hydrogen.

It is worth noting in the paper that hydrogen was not measured directly in the conducted research, but some statements were indicated that are hypothetical and worth developing scientifically. In this way, one can refer to the causal hypothesis that proposes to explain the causal relationship of an explanatory and predictive nature.

The transition from mobile equipment to methanol-based biofuel requires a careful approach to the selection of fuel material and other engine systems for mobile equipment—it should be noted that the materials most sensitive to biofuels are A0 aluminum and Br bronze.

It was found that the use of biofuels in the operation of self-propelled agricultural machinery has a negative impact on the reliability of its functional systems. Among the factors that cause a decrease in reliability are the most significant operating conditions (15–20%) and operating modes (50–60%) and the physical and chemical properties of structural materials used for the manufacture of individual elements (25–30%).

It has been proven that biodiesel is more aggressive to construction materials compared to mineral diesel fuel.

The nature and course of physicochemical phenomena, which is a specific characteristic of a specific sliding system (material associations, excitations, environment, etc.), are indicated, and not a general phenomenon common to all friction pairs. Detailed knowledge of the physicochemical phenomena occurring in the friction process is possible only when it is possible to strictly control the factors that influence the course of these phenomena.

**Author Contributions:** Conceptualization, D.Z., A.B., V.L.-L., B.B., L.B. and H.S.; data curation, D.Z., A.B., V.L.-L., B.B., L.B. and H.S.; formal analysis, D.Z., A.B., V.L.-L., B.B., L.B. and H.S.; funding acquisition, M.K., K.K., G.M. and G.W.; investigation, D.Z., A.B., V.L.-L., B.B., L.B. and H.S.; methodology, D.Z., A.B., V.L.-L., B.B., L.B., H.S., S.S., R.K., G.F. and G.W.; project administration, D.A., B.D. and G.W.; resources, M.K., K.K., G.M., S.S., R.K., G.F., D.A., B.D. and G.W.; software, D.Z., A.B., V.L.-L., B.B., L.B. and H.S.; supervision, S.S., R.K., G.F. and G.W.; validation, M.K., K.K., G.M., D.A., B.D. and G.W.; visualization, D.Z., A.B., V.L.-L., B.B., L.B., H.S.; roles/writing—original draft, D.Z., A.B., V.L.-L., B.B., L.B., H.S. and G.W.; writing—review and editing, G.W. All authors have read and agreed to the published version of the manuscript.

**Funding:** The study was conducted as part of the project financed by the National Center for Research and Development implemented under the BIOSTRATEG program, contract no. BIOSTRATEG1/269056/5/NCBR/2015 by (1) the Department of Technology in the Poznan Branch, Institute of Technology and Life Sciences-National Research Institute, Falenty in Poland and in cooperation with (2) the University of Life Sciences in Lublin in Poland, (3) the Dmytro Motornyi Tavria State Agrotechnological University in Ukraine, (4) the Lviv National Agrarian University in Ukraine, (5) the Jacob of Paradyz University in Gorzow Wielkopolski in Poland and (6) the Opole University of Technology. The APC was funded by the University of Life Sciences in Lublin.

**Institutional Review Board Statement:** Not applicable.

**Informed Consent Statement:** Not applicable.

**Data Availability Statement:** The data presented in this study are available on request from the corresponding authors.

**Conflicts of Interest:** The authors declare no conflict of interest. The funders had no role in the design of the study, in the collection, analyses, or interpretation of data, in the writing of the manuscript, or in the decision to publish the results.

## References

1. The European Commission. Innovation at the service of sustainable growth: The bioeconomy for Europe. *Comm. Commun. COM* **2012**, *60*, 3.
2. Jonek-Kowalska, I.; Berny, D.; Płaza, G. Assessment of biofuels competitiveness in the current technological, market and legal conditions. In *Scientific Papers of the Silesian University of Technology*; Series: Organization and Management; Silesian University of Technology; Faculty of Organization and Management: Gliwice, Poland, 2016; pp. 142–152.

3. Gralak, K. Bioeconomy as an area of intelligent regional specialization. *Eur. Policies Financ. Mark.* **2015**, *14*, 65–73.
4. The European Commission. Europe 2020: A strategy for smart, sustainable and inclusive growth. *Comm. Commun. COM 2020*, *2010*, 13.
5. Gołębiewski, J. Sustainable Bioeconomy-Potential and Development Factors. In Proceedings of the IX Congress of Polish Economists, Warszawa, Poland, 9 July 2013; p. 2.
6. The Knowledge Based Bio-Economy (KBBE) in Europe: Achievements and Challenges. 2010. Available online: [http://www.bioeconomy.net/reports/files/KBBE\\_2020\\_BE\\_presidency.pdf](http://www.bioeconomy.net/reports/files/KBBE_2020_BE_presidency.pdf) (accessed on 10 January 2022).
7. Maciejczak, M.; Hofreiter, K. How to define bioeconomy? *Assoc. Agric. Agribus. Econ. Ann. Sci.* **2013**, *15*, 244–246.
8. Pajewski, T. Bioeconomy as a strategic element of sustainable agriculture. *Assoc. Agric. Agribus. Econ. Ann. Sci.* **2014**, *16*, 179–184.
9. Kozłowska, A.; Kozłowski, K.; Skawiński, W.; Kapka-Skrzypczak, L. Effect of pollutants emissions from biofuels on the environment and human health. *Hygeia Public Health* **2020**, *55*, 45–55.
10. Leme, D.M.; Grummt, T.; de Oliveira, D.P.; Sehr, A.; Renz, S.; Reinel, S.; Ferraz, E.R.A.; de Marchi, M.R.R.; Machado, M.C.; Zocolo, G.J.; et al. Genotoxicity assessment of water soluble fractions of biodiesel and its diesel blends using the Salmonella assay and the in vitro MicroFlow<sup>®</sup> kit (Litron) assay. *Chemosphere* **2012**, *86*, 512–520. [[CrossRef](#)]
11. Berny, D.; Wandzich, D.; Plaza, G. Challenges for the biofuel sector in the light of the developing bioeconomy. *Sci. Pap. Sil. Univ. Technol. Organ. Manag.* **2015**, *79*, 41–55.
12. Biernat, K. Second generation biofuels. *Studia Ecol. Bioethicae* **2007**, *5*, 281–294. [[CrossRef](#)]
13. Polish Standard PN-EN 14214; Liquid Petroleum Products-Fatty Acid Methyl Esters (FAME) for Use in Compression-Ignition (Diesel) Car Engines and Heating Applications-Requirements and Test Methods. Polish Committee for Standardization: Warszawa, Poland, 2015.
14. Galwas-Zakrzewska, M.; Makles, Z. The influence of biocomponents on the composition of engine exhaust gases. *Work Saf.* **2013**, *11*, 10–13.
15. Rauch, R.; Hrbek, J.; Hofbauer, H. Biomass gasification for synthesis gas production and applications of the syngas. *Wiley Interdiscip. Rev. Energy Environ.* **2013**, *3*, 343–362. [[CrossRef](#)]
16. Rabalski, M. Biopaliwa Płynne. Available online: <https://energia360.pl/biomasa,ac149/biopaliwa-plynnne,1711> (accessed on 15 February 2017).
17. Górski, W.; Jabłońska, M.M. Dimethyl ether-universal, ecological fuel of the 21st century. *NAFTA-GAZ* **2012**, *ROK LXVIII*, 631–641.
18. Marcinkowski, D.; Gracz, W. Production of biofuels and bioproducts. In *the Monograph-Production of Biogas in a Biomass Refinery, Taking into Account the Aspects of Biogas Plant Operation*; Wawrzyniak, A., Ed.; Institute of Technology and Life Sciences: Falenty, Poland; Publishing House ITP: Warsaw, Poland, 2020.
19. Roszkowski, A. Biodiesel in the EU and Poland-current conditions and prospects. *Agric. Eng. Probl.* **2012**, *20*, 65–78.
20. Malina, R. HEFA and F-T jet fuel cost analyses. In Proceedings of the Sustainable Alternative Fuels Cost Workshop (MIT), Cambridge, MA, USA, 27 November 2012.
21. Picazo-Espinosa, R.; González-López, J.; Manzanera, M. Bioresources for Third-Generation Biofuels. Available online: [www.intechopen.com/download/pdf/17479](http://www.intechopen.com/download/pdf/17479) (accessed on 12 May 2012).
22. Błaszak, M. The use of algae for energy: Current state and perspectives. *Arch. Waste Manag. Environ. Prot.* **2014**, *16*, 141–152.
23. Szymczyk, E. The State of Research and Prospects for the Implementation of Technology for the Production of Fuel Bioethanol from Lignocellulosic Raw Materials. Ph.D. Thesis, Faculty of Energy and Fuels, AGH University of Science and Technology Stanisława Staszica, Kraków, Poland, 2008.
24. Owczuk, M. Biodiesel and environmental protection. In *Studia Ecologiae et Bioethicae*; Institute of Fuels and Renewable Energy: Warsaw, Poland, 2006; Volume 4, pp. 351–356.
25. Li, H.; Shi, L.; Deng, K. Development of turbocharging system for diesel engines of power generation application at different altitudes. *J. Energy Inst.* **2016**, *89*, 755–765. [[CrossRef](#)]
26. Shelar, M.N.; Bagade, S.D.; Kulkarni, G.N. Energy and Exergy Analysis of Diesel Engine Powered Trigeneration Systems. *Energy Proc.* **2016**, *90*, 27–37. [[CrossRef](#)]
27. Seifi, M.R.; Hassan-Beygi, S.R.; Ghobadian, B.; Desideri, U.; Antonelli, M. Experimental investigation of a diesel engine power, torque and noise emission using water–diesel emulsions. *Fuel* **2016**, *166*, 392–399. [[CrossRef](#)]
28. Mikulski, M.; Wierzbicki, S. Numerical investigation of the impact of gas composition on the combustion process in a dual-fuel compression-ignition engine. *J. Nat. Gas Sci. Eng.* **2016**, *31*, 525–537. [[CrossRef](#)]
29. Wasilewski, J.; Krzaczek, P. Emission of toxic compounds from combustion of biodiesel: A report from studies. *Przem. Chem.* **2014**, *93*, 343–346. [[CrossRef](#)]
30. Hoseini, S.S.; Najafi, G.; Ghobadian, B.; Mamat, R.; Sidik, N.A.C.; Azmi, W.H. The effect of combustion management on diesel engine emissions fueled with biodiesel-diesel blends. *Renew. Sustain. Energy Rev.* **2017**, *73*, 307–331. [[CrossRef](#)]
31. Asokan, M.; Prabu, S.S.; Kamesh, S.; Khan, W. Performance, combustion and emission characteristics of diesel engine fuelled with papaya and watermelon seed oil bio-diesel/diesel blends. *Energy* **2017**, *145*, 238–245. [[CrossRef](#)]
32. Hossain, F.M.; Rainey, T.; Ristovski, Z.; Brown, R.J. Performance and exhaust emissions of diesel engines using microalgae FAME and the prospects for microalgae HTL biocrude. *Renew. Sustain. Energy Rev.* **2018**, *82*, 4269–4278. [[CrossRef](#)]
33. Canakci, M.; Sanli, H. Biodiesel production from various feedstocks and their effects on the fuel properties. *J. Ind. Microbiol. Biotechnol.* **2008**, *35*, 431–441. [[CrossRef](#)]

34. Rehan, M.; Gardy, J.; Demirbas, A.; Rashid, U.; Budzianowski, W.M.; Pant, D.; Nizami, A.S. Waste to biodiesel: A preliminary assessment for Saudi Arabia. *Bioresour. Technol.* **2018**, *250*, 17–25. [[CrossRef](#)]
35. Sander, A.; Koščak, M.A.; Kosir, D.; Milosavljević, N.; Vuković, J.P.; Magić, L. The influence of animal fat type and purification conditions on biodiesel quality. *Renew. Energy* **2018**, *118*, 752–760. [[CrossRef](#)]
36. Matwijczuk, A.; Zając, G.; Kowalski, R.; Kachel-Jakubowska, M.; Gagoś, M. Spectroscopic Studies of the Quality of Fatty Acid Methyl Esters Derived from Waste Cooking Oil. *Pol. J. Environ. Stud.* **2017**, *26*, 2643–2650. [[CrossRef](#)]
37. Marcinkowski, D.; Rukowicz, B.; Golimowski, W.; Czechlowski, M.; Krzaczek, P.; Piekarski, W. Effect of selected depressants on cold filter plugging point for methyl esters obtained from transesterification of waste vegetable and animal fats. *Przem. Chem.* **2017**, *96*, 1927–1930. [[CrossRef](#)]
38. Krzaczek, P.; Rybak, A.; Bochniak, A. The impact of selected biofuels on the performance parameters of the Common Rail power system in the utility engine. In Proceedings of the 10th International Scientific Conference on Aeronautics, Automotive and Railway Engineering and Technologies, Sozopol, Bulgaria, 15–17 September 2018. [[CrossRef](#)]
39. Cucui, G.; Ionescu, C.A.; Goldbach, I.R.; Coman, M.D.; Marin, E.L.M. Quantifying the Economic Effects of Biogas Installations for Organic Waste from Agro-Industrial Sector. *Sustainability* **2018**, *10*, 2582. [[CrossRef](#)]
40. Pillay, A.; Molki, A.; Elkadi, M.; Manuel, J.; Bojanampati, S.; Khan, M.; Stephen, S. Real-Time Study of Noxious Gas Emissions and Combustion Efficiency of Blended Mixtures of Neem Biodiesel and Petrodiesel. *Sustainability* **2013**, *5*, 2098–2107. [[CrossRef](#)]
41. Basavarajappa, Y.H.; Banapurmath, N.R.; Pradeep, G.; Vinod, R.; Yaliwal, V. Performance and emission characteristics of a CNG-Biodiesel dual fuel operation of a single cylinder four stroke CI engine. *IOP Conf. Ser. Mater. Sci. Eng.* **2018**, *376*, 012028. [[CrossRef](#)]
42. Golimowski, W.; Krzaczek, P.; Marcinkowski, D.; Gracz, W.; Wałowski, G. Impact of Biogas and Waste Fats Methyl Esters on NO, NO<sub>2</sub>, CO, and PM Emission by Dual Fuel Diesel Engine. *Sustainability* **2019**, *11*, 1799. [[CrossRef](#)]
43. Wang, Q.; Ge, M.; Guo, X.; Li, Z.; Huang, A.; Yang, F.; Guo, R. Hydrophobic poly(ionic liquid)s as “two-handed weapons”: Maximizing lipase catalytic efficiency in transesterification of soybean oil toward biodiesel. *Appl. Catal. A Gen.* **2021**, *626*, 118350. [[CrossRef](#)]
44. Zhao, R.; Yang, X.; Li, M.; Peng, X.; Wei, M.; Zhang, X.; Yang, L.; Li, J. Biodiesel preparation from *Thlaspi arvense* L. seed oil utilizing a novel ionic liquid core-shell magnetic catalyst. *Ind. Crop. Prod.* **2021**, *162*, 113316. [[CrossRef](#)]
45. Malekghasemi, S.; Kariminia, H.-R.; Plechkova, N.K.; Ward, V.C. Direct transesterification of wet microalgae to biodiesel using phosphonium carboxylate ionic liquid catalysts. *Biomass-Bioenergy* **2021**, *150*, 106126. [[CrossRef](#)]
46. Yu, J.; Wang, Y.; Sun, L.; Xu, Z.; Du, Y.; Sun, H.; Li, W.; Luo, S.; Ma, C.; Liu, S. Catalysis Preparation of Biodiesel from Waste *Schisandra chinensis* Seed Oil with the Ionic Liquid Immobilized in a Magnetic Catalyst: Fe<sub>3</sub>O<sub>4</sub>@SiO<sub>2</sub>@[C4mim]HSO<sub>4</sub>. *ACS Omega* **2021**, *6*, 7896–7909. [[CrossRef](#)] [[PubMed](#)]
47. Naushad, M.; Ahamad, T.; Khan, M.R. Fabrication of magnetic nanoparticles supported ionic liquid catalyst for transesterification of vegetable oil to produce biodiesel. *J. Mol. Liq.* **2021**, *330*, 115648. [[CrossRef](#)]
48. Changmai, B.; Rano, R.; Vanlalveni, C.; Rokhum, L. A novel Citrus sinensis peel ash coated magnetic nanoparticles as an easily recoverable solid catalyst for biodiesel production. *Fuel* **2021**, *286*, 119447. [[CrossRef](#)]
49. Zhang, P.; Liu, P.; Fan, M.; Jiang, P.; Haryono, A. High-performance magnetite nanoparticles catalyst for biodiesel production: Immobilization of 12-tungstophosphoric acid on SBA-15 works effectively. *Renew. Energy* **2021**, *175*, 244–252. [[CrossRef](#)]
50. Roy, M.; Mohanty, K. Valorization of de-oiled microalgal biomass as a carbon-based heterogeneous catalyst for a sustainable biodiesel production. *Bioresour. Technol.* **2021**, *337*, 125424. [[CrossRef](#)]
51. Akkarawatkhosith, N.; Tongtummachat, T.; Kaewchada, A.; Jaree, A. Non-catalytic and glycerol-free biodiesel production from rice bran oil fatty acid distillate in a microreactor. *Energy Convers. Manag.* **2021**, *11*, 100096. [[CrossRef](#)]
52. Jung, S.; Jung, J.-M.; Lee, K.H.; Kwon, E.E. Biodiesels from non-catalytic transesterification of plant oils and their performances as aviation fuels. *Energy Convers. Manag.* **2021**, *244*, 114479. [[CrossRef](#)]
53. Sukharev, E.A. The operational reliability of the machines. In *Theory, Methodology, Modeling: A Tutorial*; NUVHP: Rivne, Ukraine, 2006; p. 192.
54. Voitov, V.A.; Datsenko, M.S.; Karnaukh, M.V. Features of operation of fuel equipment of agricultural diesels with use of biofuels. *Mach. Technol. Agro-Ind. Complex* **2010**, *1*, 13–18.
55. Devianin, S.N.; Markov, V.A.; Semenov, V.G. *Vegetable Oils and Fuels Based on Them for Diesel Engines*; Publishing Center of State University of Agricultural Science, Moscow State University: Moscow, Russia, 2007; p. 340.
56. Molodyk, M.V. *Scientific Bases of the System of Maintenance and Repair of Machines in Agriculture*; CODE: Kirovograd, Ukraine, 2009; p. 180.
57. Chernovol, M.I. (Ed.) *Reliability of Agricultural Machinery*, 2nd ed.; Reworked, and add; National University of Bioresources and Natural Resources of Ukraine: Kirovograd, Ukraine, 2010; p. 168.
58. Tziourtzioumis, D.; Demetriades, L.; Zogou, O.; Stamatelos, A. Experimental investigation of the effect of a B70 biodiesel blend on a common-rail passenger car diesel engine. *Proc. Inst. Mech. Eng. Part D J. Automob. Eng.* **2009**, *223*, 685–701. [[CrossRef](#)]
59. Lin, B.F.; Huang, J.H.; Huang, D.Y. Experimental study of the effects of vegetable oil methyl ester on DI diesel engine performance characteristics and pollutant emissions. *Fuel* **2009**, *88*, 1779–1785. [[CrossRef](#)]
60. Nagy, A.L.; Knaup, J.; Zsoldos, I. A friction and wear study of laboratory aged engine oil in the presence of diesel fuel and oxymethylene ether. *Tribol.-Mater. Surf. Interfaces* **2018**, *13*, 20–30. [[CrossRef](#)]

61. Singh, P.; Goel, V.; Chauhan, S.R. Effects of dual biofuel approach for total elimination of diesel on injection system by reciprocatory friction monitor. *Proc. Inst. Mech. Eng. Part J J. Eng. Tribol.* **2018**, *232*, 1068–1076. [[CrossRef](#)]
62. Zhuravel, D.P. Methodology for assessing the reliability of mobile agricultural machinery during operation on different types of fuels and lubricants. In *Bulletin of Sumy National Agrarian University*; Sumy National Agrarian University: Sumy, Ukraine, 2016; pp. 66–71.
63. Zhuravel, D.P. Increasing the durability of functional systems of agricultural machinery using biofuels and lubricants. In *Scientific Bulletin of the National University of Life and Environmental Sciences of Ukraine*; Series: Machinery and Energy of Agro-Industrial Complex. K. Sumy National Agrarian University: Sumy, Ukraine, 2018; pp. 279–292.
64. Zhuravel, D.P. Modeling of the process of wear of precision pairs of fuel systems of mobile equipment during operation on biodiesel. In *Works of TSATU*; National University of Bioresources and Natural Resources of Ukraine: Kirovograd, Ukraine, 2018; pp. 105–118.
65. Zhuravel, D.P. Improving the efficiency of mobile agricultural machinery by ensuring the optimal composition of blended biodiesel fuels. In *Scientific Bulletin of TSATU: Electronic Scientific Professional Publication*; TSATU: Melitopol, Ukraine, 2018; Issue 8, Item 2; pp. 91–107.
66. Baberg, A.; Freidhager, M.; Mergel, H.; Schmidt, K. Aspekte der Kolbenmaterialwahl bei Dieselmotoren. *Mot. Z.* **2012**, *73*, 964–969. [[CrossRef](#)]
67. Blümm, M.; Baberg, A.; Dörnenburg, F.; Leitzmann, D. Innovative Schaftbeschichtungen für Otto- und Dieselmotorkolben. *Mot. Z.* **2016**, *77*, 54–59. [[CrossRef](#)]
68. Deuss, T.; Ehnis, H.; Rose, R.; Künzel, R. Reibleistungsmessungen am Befeuereten Dieselmotor-Potenziale der Kolbengruppe. *Mot. Z.* **2010**, *71*, 326–330.
69. Mahle GmbH, *Piston and Engine Testing*; Typesetting: Klementz Publishing Services, Freiburg, Printing Company; AZ Druck und Datentechnik: Berlin/Stuttgart, Germany, 2012; ISBN 978-3-8348-1590-3; Available online: <https://link.springer.com/content/pdf/bfm%3A978-3-8348-8662-0%2F1.pdf> (accessed on 1 May 2022).
70. Wróblewski, E.; Iskra, A.; Babiak, M. Minimizing the wear of elements of the piston-cylinder group. In *Operation and Tests*; BUS-ES: Poland, 2017; p. 1137.
71. Nadolny, K.; Chmielewski, Z.; Nikoniuk, J. Non-invasive method of assessing the wear of cylinder liners of a diesel engine. In *Operation and Reliability*; 2005; pp. 30–37. Available online: <http://docplayer.pl/7170823-Spis-tresci-nauka-i-technika.html> (accessed on 1 May 2022).
72. Łuczak, A.; Mazur, T. *Physical Aging of Machine Elements*; WNT: Warsaw, Poland, 1981.
73. Nadolny, K. *Reliability Problems of Operational Changes in the Quality of Engine Lubricating Oils*; Dissertations No. 164; Poznań University of Technology: Poznań, Poland, 1985.
74. Niewczas, A.; Gil, L.; Ignaciuk, P. *Analysis of the Tribological Wear Processes of the Elements of the Injection System of a Com-Pression-Ignition Engine Fueled with Vegetable Oils*; Szczodrak, M., Kamińska, P., Konieczna, A., Eds.; WSEI Scientific Journals Series: Transport and Information Technology, 1, 1/2011, 5–22; Poland Innovatio Press Scientific Publishing House of the University of Economics and Innovation: Lublin, Poland, 2011; ISSN 2084-8005.
75. Nowiński, E.; Giemza, B.; Domański, M. Thickness measurement of thin oil layers in triboelectrical phenomenon aspect. *J. KONBiN* **2015**, *27*, 87–98. [[CrossRef](#)]
76. Kulczycki, A.; Wachal, A. Energy problems of boundary layer durability. *Tribology* **1985**, *16*, 21–23.
77. Napadłak, W. Tribological models of cooperation piston-piston rings-cylinder liner of the combustion engine. *Tribology* **2009**, *5*, 135–145.
78. Georgianni, K.G.; Kontominas, M.G.; Pomonis, P.J.; Avlonitis, D.; Gergis, V. Conventional and in situ transesterification of sunflower seed oil for the production of biodiesel. *Fuel Process. Technol.* **2008**, *89*, 503–509. [[CrossRef](#)]
79. Boltianskyi, B.; Sklyar, R.; Boltyanska, N.; Boltianska, L.; Dereza, S.; Grigorenko, S.; Syrotyuk, S.; Jakubowski, T. The Process of Operation of a Mobile Straw Spreading Unit with a Rotating Finger Body-Experimental Research. *Processes* **2021**, *9*, 1144. [[CrossRef](#)]
80. Dobrzański, L.A.; Dobrzańska-Danikiewicz, A.D. Changes in the structure and surface properties of engineering materials as a result of exploitation. Subsection: 8.1. General classification of changes in the structure and surface properties of engineering materials as a result of exploitation. *Open Access Libr.* **2011**, *5*, 368–416.
81. Płaza, S.; Margielewski, L.; Celichowski, G. *Introduction to Tribology and Tribochemistry*; Publishing House of the University of Lodz: Lodz, Poland, 2005; ISBN 83-7171-909-4.
82. Hadam, U.; Zakroczyński, T. Stress and strain in hydrogen embrittlement of metals. *Prot. Against Corros.* **2010**, *4–5*, 239–241.
83. Pietkun-Greber, I.; Janka, R.M. Effect of hydrogen on metals and alloys. *Proc. ECOPole* **2010**, *4*, 471–476.
84. Łunarska, E. Hydrogen corrosion in industrial installations and pipelines. Its monitoring and prevention. In *Proceedings of the Mater. IV National Corrosion Conference KORozJA'93, IChF PAN, Warsaw, Poland, 1993*; pp. 8–13.
85. Zakroczyński, T. Modification of metal surfaces to prevent hydrogen corrosion. *Prot. Against Corros.* **2006**, *4*, 99–102.
86. Chen, J.-M.; Wu, J.-K. Hydrogen diffusion through copper-plated AISI 4140 steels. *Corros. Sci.* **1992**, *33*, 657–666. [[CrossRef](#)]
87. Flis, J. Penetration of hydrogen into steel with a modified surface layer. *Prot. Against Corros.* **2000**, *7*, 177–179.
88. Zakroczyński, T. Methods of preventing the absorption of hydrogen by metals. *Prot. Against Corros.* **2005**, *4*, 90–93.

89. CORDIS. Available online: <https://cordis.europa.eu/article/id/92756-hydrogen-transport-in-metals-understood/pl> (accessed on 1 April 2022).
90. Kračun, A.T.; Zobov, E.V.; Morar, V.E.; Bruchis, M.M.; Kračun, S.V. Issledovanie vlijanija tverdogo smazočnogo materiala na protivoznosnye, protivozadirnye i antifrikcionnye svojstva plastičnych smazok. *Trenie Iznos* **1981**, *2*, 856–863.
91. Krawiec, S. *Compositions of Plastic and Solid Lubricants in the Process of Friction of Steel Machine Nodes*; Publishing House of the Wrocław University of Technology: Wrocław, Poland, 2011; ISBN 978-83-7493-658-3.
92. Nowak, J. Influence of Batch Leads on the Microstructure and Selected Properties of Ductile Iron Smelted at a Given Superheating Temperature. Ph.D. Thesis, Faculty of Foundry Engineering, AGH University of Science and Technology Stanisława Staszica, Kraków, Poland, 2019. Available online: <https://winntbg.bg.agh.edu.pl/rozprawy2/11464/full11464.pdf> (accessed on 1 April 2022).
93. Zander, D. Hydrogen Gas Pressure Regulation to 16 Bar Using Aluminum Materials. Available online: <https://www.medenus.de/files/upload/downloads/wasserstoff/medenus-regulacja-cisnienia-gazu-wodorowego.pdf> (accessed on 1 April 2022).
94. Niekurzak, M. Determining the Unit Values of the Allocation of Greenhouse Gas Emissions for the Production of Biofuels in the Life Cycle. *Energies* **2021**, *14*, 8394. [[CrossRef](#)]
95. Niekurzak, M. The Potential of Using Renewable Energy Sources in Poland Taking into Account the Economic and Ecological Conditions. *Energies* **2021**, *14*, 7525. [[CrossRef](#)]
96. Adams, P.W.; McManus, M.C. Characterisation and variability of greenhouse gas emissions from biomethane production via anaerobic digestion of maize. *J. Clean. Prod.* **2019**, *218*, 529–542. [[CrossRef](#)]
97. Olczak, P.; Matuszewska, D.; Kryzia, D. “Mój Prąd” as an example of the photovoltaic one off grant program in Poland. *Energy Policy J.* **2020**, *23*, 123–138. [[CrossRef](#)]
98. Niekurzak, M.; Kubińska-Jabcoń, E. Analysis of the return on investment in solar collectors on the example of a household: The case of Poland. *Front. Energy Res.* **2021**, *9*, 660140. [[CrossRef](#)]
99. Ledakowicz, S.; Krzystek, L. Wykorzystanie fermentacji metanowej w utylizacji odpadów przemysłu rolno-spożywczego. *Biotechnologia* **2005**, *3*, 165–183.
100. Ardolino, F.; Parrillo, F.; Arena, U. Biowaste-to-biomethane or biowaste-to-energy? An LCA study on anaerobic digestion of organic waste. *J. Clean. Prod.* **2018**, *174*, 462–476. [[CrossRef](#)]
101. Kalina, J.; Skorek, J.; Cebula, J.; Latocha, L. Pozyskiwanie i energetyczne wykorzystanie biogazu rolniczego. *Gospod. Paliwami Energią* **2003**, *12*, 14–19.
102. Ge, J.; Choi, N. Soot Particle Distribution and Regulated and Unregulated Emissions of a Diesel Engine Fueled with Palm Oil Biodiesel Blends. *Energies* **2020**, *13*, 5736. [[CrossRef](#)]
103. Ge, J.C.; Kim, H.Y.; Yoon, S.K.; Choi, N.J. Reducing volatile organic compound emissions from diesel engines using canola oil biodiesel fuel and blends. *Fuel* **2018**, *218*, 266–274. [[CrossRef](#)]
104. Ge, J.C.; Kim, H.Y.; Yoon, S.K.; Choi, N.J. Optimization of palm oil biodiesel blends and engine operating parameters to improve performance and PM morphology in a common rail direct injection diesel engine. *Fuel* **2020**, *260*, 116326. [[CrossRef](#)]
105. Voytovych, I.; Malovanyy, M.; Zhuk, V.; Mukha, O. Facilities and problems of processing organic wastes by family-type bio-gas plants in Ukraine. *J. Water Land Dev.* **2020**, *45*, 185–189. [[CrossRef](#)]
106. Wałowski, G. Development of biogas and biorafinery systems in Polish rural communities. *J. Water Land Dev.* **2021**, *49*, 156–168. [[CrossRef](#)]
107. Awogbemi, O.; Kallon, D.V.V.; Onuh, E.I.; Aigbodion, V.S. An Overview of the Classification, Production and Utilization of Biofuels for Internal Combustion Engine Applications. *Energies* **2021**, *14*, 5687. [[CrossRef](#)]
108. Directive 2009/28/EC of the European Parliament and of the Council of 23 April 2009. On the Promotion of the Use of Energy from Renewable Sources Amending and Subsequently Repealing Directives 2001/77/EC and 2003/30/EC. Available online: <https://eur-lex.europa.eu/legal-content/EN/TXT/PDF/?uri=CELEX:32009L0028> (accessed on 1 April 2022).
109. Directive 2012/27/EU of the European Parliament and of the Council of 25 October 2012. On Energy Efficiency, Amending Directives 2009/125/EC and 2010/30/EU and Repealing Directives 2004/8/EC and 2006/32/EC. Available online: <https://eur-lex.europa.eu/legal-content/EN/NIM/?uri=celex:32012L0027> (accessed on 1 April 2022).